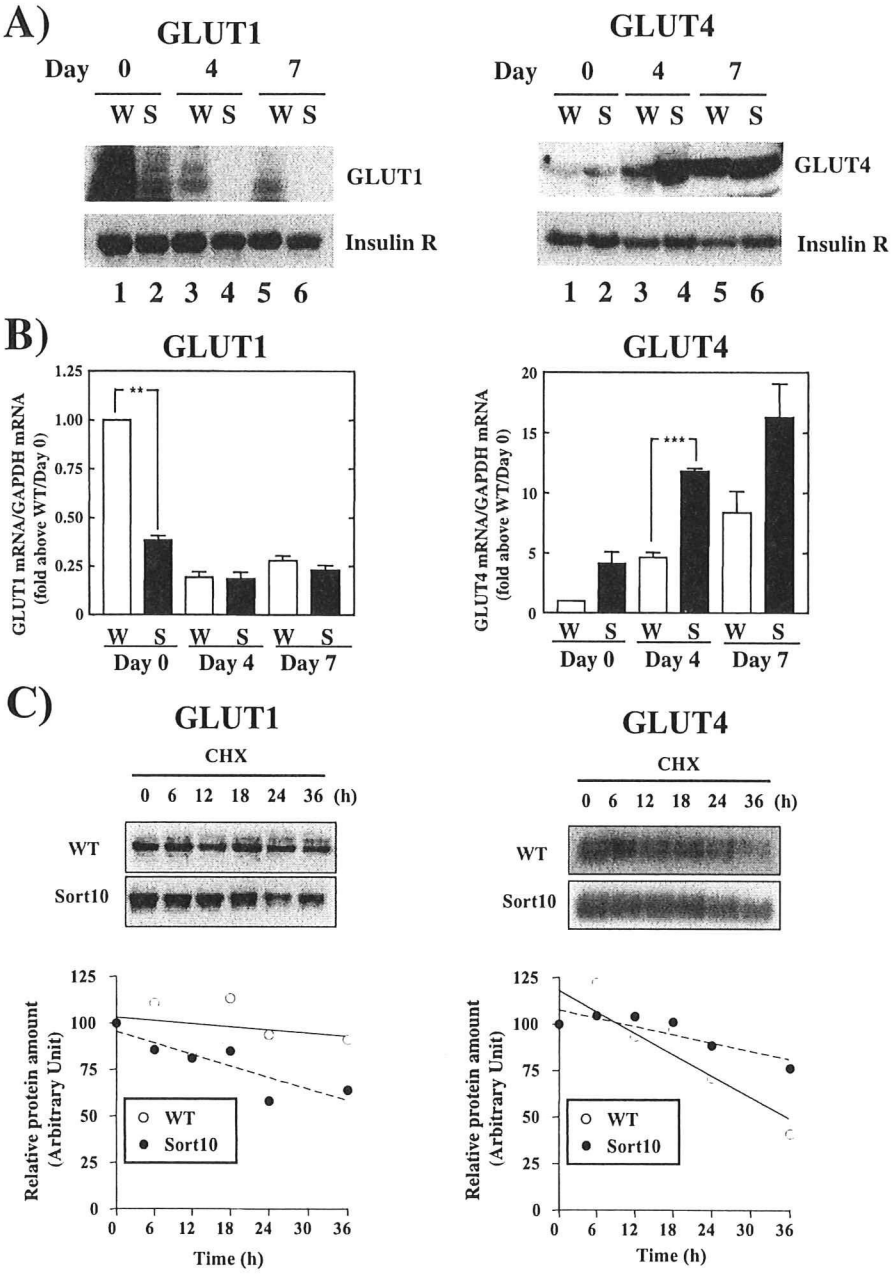

FIGURE 6. **Effect of sortilin overexpression on the protein and mRNA levels of GLUT1 and GLUT4 in C2C12 cells.** *A*, total membrane fractions were obtained from WT-C2C12 cells (*lanes 1, 3,* and *5*) and Sort10-C2C12 cells (*lanes 2, 4,* and *6*) at Day 0 (*lanes 1* and *2*), Day 4 (*lanes 3* and *4*), and Day 7 (*lanes 5* and *6*) of differentiation, as described under "Experimental Procedures." Protein extracts from total membranes (120 μg/lane) were subjected to SDS-PAGE followed by Western blotting using antibodies against GLUT1 (*left panel*) or GLUT4 (*right panel*). *B*, total RNA was isolated from WT-C2C12 cells (*open bars*) and Sort10-C2C12 cells (*solid bars*) on the indicated day after differentiation. The relative abundances of mRNAs for GLUT1 (*left graph*) and GLUT4 (*right graph*) were evaluated by real-time PCR analysis. Data normalized using the glyceraldehyde-3-phosphate dehydrogenase (*GAPDH*) transcript were averaged over three independent experiments and are shown as -fold changes over Day 0 in WT-C2C12 cells. *C*, time dependent changes in protein amounts of GLUT1 (*left panels*) and Myc-GLUT4-ECFP (*right panels*) after addition of 10 μg/ml cycloheximide were monitored in WT (*open circles*) and Sort10 (*closed circles*) C2C12 cells by Western blotting.

bars) as compared with WT-C2C12 cells (*open bars*), whereas expression levels of Ubc9 mRNA decreased upon differentiation in both WT- and Sort10-C2C12 cells. As a result of the increased Ubc9 in Sort10-C2C12 cells, SUMO-modified proteins were also increased (Fig. 7*A*, *right panel*, *lanes 2, 4,* and *6*).

DISCUSSION

Although substantial progress has been made in our understanding of the insulin-induced GLUT4 translocation process in adipocytes, achieved mainly using the excellent 3T3L1 adipogenic cell culture model (46), much less information is available about the mechanistic details involved in this event in skeletal muscle, the tissue in which the effect of insulin on glucose disposal is quantitatively most important. Recently, we have reported that, much like the L6 skeletal muscle cell line, a C2C12 myogenic cell line derived from mouse skeletal muscle possesses the basic machinery required for GLUT4 translocation in response to insulin stimulation (43, 47). However, the insulin-induced glucose uptake achieved by this GLUT4 translocation is masked by relatively high basal glucose transport activity, presumably mediated through GLUT1 (35). Because it would be highly desirable to establish cell culture models of skeletal muscle that clearly and accurately reflect muscle glucose disposal *in vivo*, we have attempted to further characterize the molecular details underlying development of the insulin-induced glucose transport system in these C2C12 cells. We therefore explored the functional roles of sortilin, a sorting receptor implicated in the formation of insulin-responsive GLUT4 vesicles in adipocytes (12, 48), by using C2C12 myocytes.

A key finding of the present studies is that sortilin functions as a potent differentiation regulator for C2C12 skeletal muscle cells, at least in part by modulating the p75NTR-proNGF autocrine loop (Figs. 2 and 3). As previously demonstrated in adipocytes (12), sortilin overexpression apparently improves the insulin-induced glucose uptake in C2C12 myocytes (Figs. 4 and 5), a novel observation that, however, reveals that this effect of sortilin on the development of

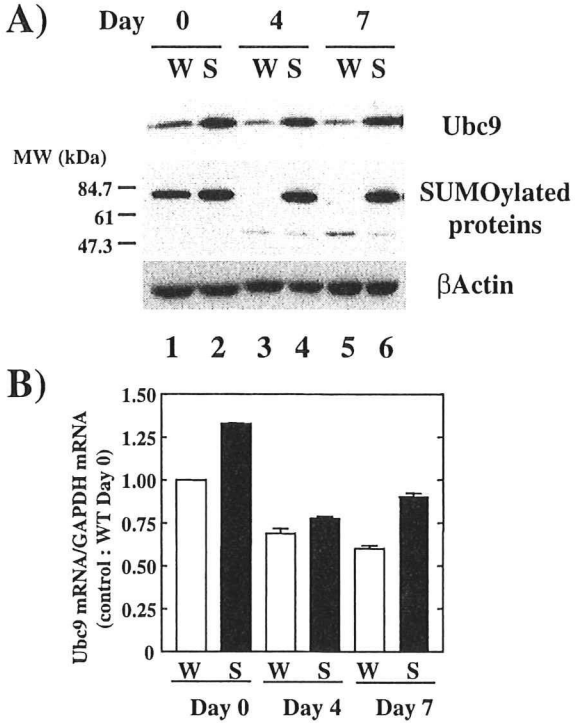

FIGURE 7. **Sortilin overexpression increases Ubc9 resulting in the accumulation of SUMO-modified proteins in C2C12 cells.** *A*, whole cell lysates were obtained from WT-C2C12 cells (*lanes 1, 3,* and *5*) and Sort10-C2C12 cells (*lanes 2, 4,* and *6*) at Day 0 (*lanes 1* and *2*), Day 4 (*lanes 3* and *4*), and Day 7 (*lanes 5* and *6*) of differentiation. Protein extracts (25 μg/lane) were subjected to SDS-PAGE followed by Western blotting using antibodies against anti-Ubc9 (*upper panel*), anti-GMP1 (SUMO-1) (*middle panel*), or anti-β-actin (*lower panel*). *B*, total RNA was isolated from WT-C2C12 cells (*open bars*) and Sort10-C2C12 cells (*solid bars*) on the indicated day after differentiation. The relative abundance of mRNAs for Ubc9 was evaluated by real-time PCR analysis. Data normalized using the glyceraldehyde-3-phosphate dehydrogenase (*GAPDH*) transcript were averaged over three independent experiments and are shown as -fold changes over Day 0 in WT-C2C12 cells.

insulin-responsiveness in C2C12 cells reflects a combination of consequences of its myogenic stimulatory action. Indeed, sortilin overexpression significantly stimulates C2C12 differentiation (Fig. 2) and thereby raises the cellular content of GLUT4 and decreases that of GLUT1 by altering both transcriptional and post-transcriptional levels (Fig. 6). Importantly, the differentiation-dependent expression of endogenous sortilin (Fig. 1) appears to be directly involved in the process of myogenesis, because siRNA-mediated suppression of sortilin significantly inhibited C2C12 differentiation (Fig. 3*C*), which is at least in part mediated through the p75NTR-NGF autocrine loop (Fig. 3*D*). In addition, we found that cellular contents of Ubc9 and SUMO-modified proteins are remarkably increased by sortilin overexpression (Fig. 7). Although it is not clear from the present study whether the up-regulated Ubc9 is directly responsible for post-translational regulation of GLUT proteins as previously reported (45), we observed that GLUT4 became more stable, whereas GLUT1 became less stable, in sortilin-overexpressing C2C12 cells (Fig. 6*C*).

Sortilin Serves as a Stimulator of C2C12 Myogenic Differentiation via Activation of the p75NTR-proNGF Autocrine Loop—In cultured myoblasts, including mouse C2C12 cells and rat L6 cells, serum withdrawal initiates the myogenic differentiation program, and it is generally accepted that autocrine/paracrine actions of insulin-like growth factors in response to serum withdrawal play an important role in the process of muscle differentiation (49, 50). In addition to the insulin-like growth factor-mediated autocrine system, several lines of evidence have demonstrated that NGF, and presumably its unprocessed form termed proNGF, is also involved in the initiation of muscle differentiation in an autocrine fashion (26, 27, 51). Furthermore, overexpression of p75NTR, a low affinity receptor for various neurotrophins, including proNGF, proBDNF, NGF, and BDNF, has been shown to induce spontaneous myogenic differentiation in a growth medium (26), which is similar to what we have observed in C2C12 myoblasts overexpressing sortilin (Fig. 2). Because p75NTR appeared to form a complex with sortilin creating high affinity receptors for proNGF and thereby evoking an intracellular signaling cascade (22), we hypothesized that sortilin overexpression allows endogenous p75NTR to respond to limiting concentrations of neurotrophins being secreted by C2C12 cells in an autocrine manner and/or fed with medium containing fetal bovine serum. Consistent with this idea, neutralizing antibodies against either p75NTR or NGF significantly inhibited the spontaneous differentiation of Sort10-C2C12 cells overexpressing sortilin (Fig. 3*A*). In addition, sortilin overexpression resulted in an efficient endocytosis of the anti-p75NTR antibody from culture media (Fig. 3*B*), suggesting that exogenously expressed sortilin facilitates formation of the functional tripartite complex composed of proNGF, p75NTR, and sortilin, as previously reported (22). More importantly, either siRNA-mediated suppression of endogenous sortilin expression or specific antibody-mediated neutralization of endogenous p75NTR/proNGF significantly inhibits low serum-induced C2C12 differentiation (Fig. 3, *C* and *D*). Together, these data demonstrate that sortilin serves as a stimulator of C2C12 myogenic differentiation mediated through potentiation of the p75NTR-proNGF autocrine loop, and that differentiation-dependent increases in endogenous sortilin participate directly in the promotion of myogenesis. It remains to be clarified whether sortilin has a similar capability in the process of adipocyte differentiation, which is currently under investigation.

It has been reported that sortilin binds mature NGF with low affinity ($K_d = 10^{-8}$ M) and proNGF with high affinity ($K_d = 10^{-9}$ M), and that the latter affinity is further increased ($K_d = 10^{-10}$ M) when sortilin associates with p75NTR (22). Therefore, our data raise the novel possibility that levels of sortilin expression regulate myogenic differentiation by modulating the biological actions mediated through the p75NTR-proNGF autocrine loop. Because sortilin expression is up-regulated (Fig. 1), whereas p75NTR and NGF expressions are down-regulated (26), upon differentiation, fine-tuning of the expression levels of these proteins would be required for proper development and maintenance of healthy muscle tissues (28). Although the signaling cascades involved in its myogenic actions have yet to be clarified, several lines of evidence indicate a signaling relationship between p75NTR and the Rho family of small GTP-binding proteins in the process of cellular differentiation (40,

41). In this regard, regulation of Rho family members has been directly implicated in myogenesis (52, 53), and the inhibition of ROCK by either Y29632 or siRNA-mediated gene silencing reportedly potentiated myogenesis of C2C12 cells (54–56). In the present study, however, we found that Y29632 significantly inhibited the myogenin expression observed in sortilin-overexpressing C2C12 cells early in differentiation (Day 0) (Fig. 3*E*). Since fine-tuning of both Rho family members and ROCK has been shown to be important for myogenesis (54–56), the precise molecular mechanisms underlying the phenomena mentioned above remain to be clarified. However, our results strongly suggest an involvement of ROCK in the potentiation of myogenesis induced by sortilin overexpression.

Effects of Sortilin Expression on the Insulin-responsive Glucose Transport System in C2C12—Sortilin is expressed in a number of tissues, including the brain, testis, and fat, as well as in skeletal muscle and the heart (17, 18, 57). Sortilin has been shown to play an important role in *trans*-Golgi network-to-endosome and *trans*-Golgi network-to-lysosome trafficking events (15). Like cation-independent mannose 6-phosphate/insulin-like growth factor-2 receptor, a well known sorting receptor that traffics among the *trans*-Golgi network, lysosomes, and the plasma membrane, sortilin possesses a short cytoplasmic tail at the C-terminal containing an acidic cluster-dileucine motif that is specifically recognized by the recently identified adaptor proteins termed GGAs (15, 58). In the context of GLUT4 regulation in adipocytes, sortilin expression is up-regulated during 3T3L1 adipocyte differentiation (18, 19), and recent studies by Kandror and colleagues demonstrated a crucial role of sortilin in the formation of insulin-sensitive GLUT4 storage vesicles responsible for the insulin-stimulated glucose transport in 3T3L1 adipocytes (12, 48). Although the precise molecular mechanism involved in the formation of insulin-responsive GLUT4 storage compartments remains largely unknown, the available evidence indicates that sortilin induces the biogenesis of vesicles containing GLUT4 in concert with GGA adaptor proteins in cultured adipocytes (59, 60). More recently, the importance of luminal interactions between sortilin and GLUT4 in endosomes for producing insulin-responsive GLUT4 storage vesicles has been demonstrated (48).

Similar to observations in the 3T3L1 adipogenic cell line (18, 19), our results demonstrate that sortilin is up-regulated upon C2C12 differentiation but is only partially colocalized to GLUT4-containing endosomes (Fig. 1). It should be noted, however, that subcellular organelles underwent a profound reorganization during myogenic differentiation, and their localization patterns and architectures differed remarkably between undifferentiated mononuclear myoblasts and differentiated multinuclear myotubes (8, 61). However, the amount of endogenous sortilin seems to be insufficient for conferring any apparent insulin-responsiveness in terms of glucose uptake in C2C12 myotubes, because insulin stimulation of 2-deoxy[^{3}H]glucose uptake was marginal (Fig. 4*B*), due to a relatively high level of basal glucose uptake mediated through GLUT1. Consistent with previous studies using fibroblastic cell types (12, 48), overexpression of sortilin in myocytes apparently produced insulin-responsiveness as assessed by both the 2-deoxy[^{3}H]glucose uptake assay (Fig. 4) and the Myc Ab uptake assay (Fig. 5). These results support the suggestion of Kandror and colleagues that sortilin plays an essential role in the development of GLUT4 storage vesicles and responsiveness to insulin (12, 48).

However, our aforementioned novel observation that sortilin overexpression significantly potentiates myogenesis sets the stage for an alternative hypothesis that sortilin participates in development of the entire insulin-responsive glucose transport system, being involved in more than just GLUT4 storage compartments, and that this is achieved, at least in part, via its myogenic stimulatory actions. This hypothesis is supported by evidence that sortilin overexpression strongly stimulates expression of the GLUT4 gene while inhibiting that of the GLUT1 gene, leading to opposite changes in GLUT4 and GLUT1 abundance (Fig. 6), which thereby produces lower basal glucose uptake and greater augmentation of glucose uptake in response to insulin (Fig. 4). In addition, emergence of the insulin-responsive glucose uptake in skeletal muscle cells by sortilin overexpression appeared to have resulted, at least in part, from the marked reduction in basal glucose uptake (Fig. 4) due to significantly reduced GLUT1 contents (Fig. 6). In this regard, we observed the half-lives of GLUT proteins to be reciprocally regulated in sortilin-overexpressing C2C12 cells (Fig. 6*C*). Thus, these data indicate sortilin to be involved not only in generating insulin-responsive GLUT4 storage vesicles, but also in elaborating the entire glucose transport system exhibiting enhanced insulin-responsiveness via regulation of the processes of myogenesis including expressions of GLUT proteins and also perhaps various other proteins involved in the development of insulin-responsiveness.

Another interesting observation presented in this study is that sortilin overexpression resulted in significant increases in the contents of Ubc9 and SUMO-modified proteins in C2C12 cells (Fig. 7). Ubc9 is the only protein serving as an E2-type SUMO-conjugating enzyme in vertebrates, and most of the well known Ubc9 interacting proteins are nuclear or are translocated to the nucleus (62, 63). Intriguingly, however, Ubc9 has been shown to interact directly with GLUT1 and GLUT4 and to modulate their membrane expression levels in opposite directions through a post-translational mechanism (45). Namely, overexpression of Ubc9 in the L6 skeletal muscle cell line results in a marked decrease in the cellular GLUT1 content and an increase in the GLUT4 content (45), which is in excellent agreement with our present results, shown in Figs. 6 and 7. Thus, the effects of sortilin overexpression on the significant reduction in cellular GLUT1 content, despite similar expression levels of its gene (Fig. 6, *A* and *B*, Days 4 and 7), may have resulted from the post-translational regulation of GLUT1 governed by the accumulated Ubc9 (Fig. 7). Although possible involvement of the accumulated Ubc9 in the increase in GLUT4 protein is not clear at this time, because it coincides with up-regulation of GLUT4 gene expression in response to sortilin overexpression (Fig. 6, *A* and *B*, *right panels*), a recent

report demonstrated that Ubc9 overexpression results in the inhibition of GLUT4 degradation and promotes its targeting to insulin-responsive GLUT4 storage compartments (64). However, another recent report demonstrated that Ubc9 is also directly involved in the myogenic differentiation of C12C12 cells (65). Thus, Ubc9 seems to have dual functions, and our observations suggest that the sortilin-induced opposite changes in GLUT4 and GLUT1 abundance might reflect a combination of the consequences of the accumulation of Ubc9, which may regulate the half-lives of GLUT proteins and also further participate in the potentiation of myogenesis. Although the degree to which sortilin actions on myogenesis or the opposite changes in GLUT1 and GLUT4 abundance, possibly mediated through Ubc9 accumulation, contributes to enhanced insulin-responsiveness is an important question warranting further research, our findings clearly provide novel insights into the functional roles of sortilin in development of the insulin-responsive glucose uptake system in muscle cells.

Acknowledgments—We thank Dr. H. Shibata (Gunma University) for providing anti-GLUT4 antibody and Dr. H. Mizuguchi (National Institute of Biomedical Innovation) for providing the pHMCA5 plasmid. We also thank Natsumi Emoto and Fumie Wagatsuma for excellent technical assistance.

REFERENCES

1. DeFronzo, R. A., Jacot, E., Jequier, E., Maeder, E., Wahren, J., and Felber, J. P. (1981) *Diabetes* **30,** 1000–1007
2. Nuutila, P., Knuuti, M. J., Raitakari, M., Ruotsalainen, U., Teras, M., Voipio-Pulkki, L. M., Haaparanta, M., Solin, O., Wegelius, U., and Yki-Jarvinen, H. (1994) *Am. J. Physiol.* **267,** E941–E946
3. Koistinen, H. A., and Zierath, J. R. (2002) *Ann. Med.* **34,** 410–418
4. Mueckler, M. (1990) *Diabetes* **39,** 6–11
5. Mitsumoto, Y., Burdett, E., Grant, A., and Klip, A. (1991) *Biochem. Biophys. Res. Commun.* **175,** 652–659
6. Shimokawa, T., Kato, M., Ezaki, O., and Hashimoto, S. (1998) *Biochem. Biophys. Res. Commun.* **246,** 287–292
7. Rodnick, K. J., Slot, J. W., Studelska, D. R., Hanpeter, D. E., Robinson, L. J., Geuze, H. J., and James, D. E. (1992) *J. Biol. Chem.* **267,** 6278–6285
8. Ralston, E., and Ploug, T. (1996) *J. Cell Sci.* **109,** 2967–2978
9. Rudich, A., and Klip, A. (2003) *Acta Physiol. Scand.* **178,** 297–308
10. Garcia de Herreros, A., and Birnbaum, M. J. (1989) *J. Biol. Chem.* **264,** 9885–9890
11. Haney, P. M., Slot, J. W., Piper, R. C., James, D. E., and Mueckler, M. (1991) *J. Cell Biol.* **114,** 689–699
12. Shi, J., and Kandror, K. V. (2005) *Dev Cell* **9,** 99–108
13. Baumann, C. A., Ribon, V., Kanzaki, M., Thurmond, D. C., Mora, S., Shigematsu, S., Bickel, P. E., Pessin, J. E., and Saltiel, A. R. (2000) *Nature* **407,** 202–207
14. Chiang, S. H., Baumann, C. A., Kanzaki, M., Thurmond, D. C., Watson, R. T., Neudauer, C. L., Macara, I. G., Pessin, J. E., and Saltiel, A. R. (2001) *Nature* **410,** 944–948
15. Nielsen, M. S., Madsen, P., Christensen, E. I., Nykjaer, A., Gliemann, J., Kasper, D., Pohlmann, R., and Petersen, C. M. (2001) *EMBO J.* **20,** 2180–2190
16. Lefrancois, S., Zeng, J., Hassan, A. J., Canuel, M., and Morales, C. R. (2003) *EMBO J.* **22,** 6430–6437
17. Petersen, C. M., Nielsen, M. S., Nykjaer, A., Jacobsen, L., Tommerup, N., Rasmussen, H. H., Roigaard, H., Gliemann, J., Madsen, P., and Moestrup, S. K. (1997) *J. Biol. Chem.* **272,** 3599–3605
18. Lin, B. Z., Pilch, P. F., and Kandror, K. V. (1997) *J. Biol. Chem.* **272,** 24145–24147
19. Morris, N. J., Ross, S. A., Lane, W. S., Moestrup, S. K., Petersen, C. M., Keller, S. R., and Lienhard, G. E. (1998) *J. Biol. Chem.* **273,** 3582–3587
20. Nielsen, M. S., Jacobsen, C., Olivecrona, G., Gliemann, J., and Petersen, C. M. (1999) *J. Biol. Chem.* **274,** 8832–8836
21. Mazella, J., Zsurger, N., Navarro, V., Chabry, J., Kaghad, M., Caput, D., Ferrara, P., Vita, N., Gully, D., Maffrand, J. P., and Vincent, J. P. (1998) *J. Biol. Chem.* **273,** 26273–26276
22. Nykjaer, A., Lee, R., Teng, K. K., Jansen, P., Madsen, P., Nielsen, M. S., Jacobsen, C., Kliemannel, M., Schwarz, E., Willnow, T. E., Hempstead, B. L., and Petersen, C. M. (2004) *Nature* **427,** 843–848
23. Teng, H. K., Teng, K. K., Lee, R., Wright, S., Tevar, S., Almeida, R. D., Kermani, P., Torkin, R., Chen, Z. Y., Lee, F. S., Kraemer, R. T., Nykjaer, A., and Hempstead, B. L. (2005) *J. Neurosci.* **25,** 5455–5463
24. Mazella, J. (2001) *Cell Signal* **13,** 1–6
25. Bronfman, F. C., and Fainzilber, M. (2004) *EMBO Rep.* **5,** 867–871
26. Seidl, K., Erck, C., and Buchberger, A. (1998) *J. Cell. Physiol.* **176,** 10–21
27. Erck, C., Meisinger, C., Grothe, C., and Seidl, K. (1998) *J. Cell. Physiol.* **176,** 22–31
28. Reddypalli, S., Roll, K., Lee, H. K., Lundell, M., Barea-Rodriguez, E., and Wheeler, E. F. (2005) *J. Cell. Physiol.* **204,** 819–829
29. Shibata, H., Suzuki, Y., Omata, W., Tanaka, S., and Kojima, I. (1995) *J. Biol. Chem.* **270,** 11489–11495
30. Yaffe, D., and Saxel, O. (1977) *Nature* **270,** 725–727
31. Onishi, M., Kinoshita, S., Morikawa, Y., Shibuya, A., Phillips, J., Lanier, L. L., Gorman, D. M., Nolan, G. P., Miyajima, A., and Kitamura, T. (1996) *Exp. Hematol.* **24,** 324–329
32. Kanzaki, M., Furukawa, M., Raab, W., and Pessin, J. E. (2004) *J. Biol. Chem.* **279,** 30622–30633
33. Mizuguchi, H., and Kay, M. A. (1998) *Hum Gene Ther.* **9,** 2577–2583
34. Mizuguchi, H., and Kay, M. A. (1999) *Hum Gene Ther.* **10,** 2013–2017
35. Nedachi, T., and Kanzaki, M. (2006) *Am. J. Physiol.* **291,** E817–E828
36. Tortorella, L. L., and Pilch, P. F. (2002) *Am. J. Physiol.* **283,** E514–E524
37. Shibata, H., Omata, W., Suzuki, Y., Tanaka, S., and Kojima, I. (1996) *J. Biol. Chem.* **271,** 9704–9709
38. Zeng, J., Hassan, A. J., and Morales, C. R. (2004) *Mol. Reprod. Dev.* **68,** 469–475
39. Peters, E. M., Stieglitz, M. G., Liezman, C., Overall, R. W., Nakamura, M., Hagen, E., Klapp, B. F., Arck, P., and Paus, R. (2006) *Am. J. Pathol.* **168,** 221–234
40. Yamashita, T., and Tohyama, M. (2003) *Nat. Neurosci.* **6,** 461–467
41. Passino, M. A., Adams, R. A., Sikorski, S. L., and Akassoglou, K. (2007) *Science* **315,** 1853–1856
42. Kanzaki, M., and Pessin, J. E. (2001) *J. Biol. Chem.* **276,** 42436–42444
43. Mitsumoto, Y., and Klip, A. (1992) *J. Biol. Chem.* **267,** 4957–4962
44. Santalucia, T., Camps, M., Castello, A., Munoz, P., Nuel, A., Testar, X., Palacin, M., and Zorzano, A. (1992) *Endocrinology* **130,** 837–846
45. Giorgino, F., de Robertis, O., Laviola, L., Montrone, C., Perrini, S., McCowen, K. C., and Smith, R. J. (2000) *Proc. Natl. Acad. Sci. U. S. A.* **97,** 1125–1130
46. Kanzaki, M. (2006) *Endocr. J.* **53,** 267–293
47. Walker, P. S., Ramlal, T., Sarabia, V., Koivisto, U. M., Bilan, P. J., Pessin, J. E., and Klip, A. (1990) *J. Biol. Chem.* **265,** 1516–1523
48. Shi, J., and Kandror, K. V. (2007) *J. Biol. Chem.* **282,** 9008–9016
49. Florini, J. R., Magri, K. A., Ewton, D. Z., James, P. L., Grindstaff, K., and Rotwein, P. S. (1991) *J. Biol. Chem.* **266,** 15917–15923
50. Florini, J. R., Ewton, D. Z., and Coolican, S. A. (1996) *Endocr. Rev.* **17,** 481–517
51. Rende, M., Brizi, E., Conner, J., Treves, S., Censier, K., Provenzano, C., Taglialatela, G., Sanna, P. P., and Donato, R. (2000) *Int. J. Dev. Neurosci.* **18,** 869–885
52. Takano, H., Komuro, I., Oka, T., Shiojima, I., Hiroi, Y., Mizuno, T., and Yazaki, Y. (1998) *Mol. Cell. Biol.* **18,** 1580–1589
53. Charrasse, S., Meriane, M., Comunale, F., Blangy, A., and Gauthier-Rouviere, C. (2002) *J. Cell Biol.* **158,** 953–965
54. Nishiyama, T., Kii, I., and Kudo, A. (2004) *J. Biol. Chem.* **279,** 47311–47319
55. Charrasse, S., Comunale, F., Grumbach, Y., Poulat, F., Blangy, A., and Gauthier-Rouviere, C. (2006) *Mol. Biol. Cell* **17,** 749–759

56. Castellani, L., Salvati, E., Alema, S., and Falcone, G. (2006) *J. Biol. Chem.* **281,** 15249–15257
57. Hermans-Borgmeyer, I., Hermey, G., Nykjaer, A., and Schaller, C. (1999) *Brain Res. Mol. Brain Res.* **65,** 216–219
58. Shiba, T., Takatsu, H., Nogi, T., Matsugaki, N., Kawasaki, M., Igarashi, N., Suzuki, M., Kato, R., Earnest, T., Nakayama, K., and Wakatsuki, S. (2002) *Nature* **415,** 937–941
59. Watson, R. T., Khan, A. H., Furukawa, M., Hou, J. C., Li, L., Kanzaki, M., Okada, S., Kandror, K. V., and Pessin, J. E. (2004) *EMBO J.* **23,** 2059–2070
60. Li, L. V., and Kandror, K. V. (2005) *Mol. Endocrinol.* **19,** 2145–2153
61. Ralston, E. (1993) *J. Cell Biol.* **120,** 399–409
62. Melchior, F. (2000) *Annu. Rev. Cell Dev. Biol.* **16,** 591–626
63. Wilson, V. G., and Rangasamy, D. (2001) *Exp. Cell Res.* **271,** 57–65
64. Liu, L. B., Omata, W., Kojima, I., and Shibata, H. (2007) *Diabetes* **56,** 1977–1985
65. Riquelme, C., Barthel, K. K., Qin, X. F., and Liu, X. (2006) *Exp. Cell Res.* **312,** 2132–2141

Impact of Plasma Oxidized Low-Density Lipoprotein Removal on Atherosclerosis

Yasushi Ishigaki, MD, PhD*; Hideki Katagiri, MD, PhD*; Junhong Gao, MD, PhD*; Tetsuya Yamada, MD, PhD; Junta Imai, MD, PhD; Kenji Uno, MD, PhD; Yutaka Hasegawa, MD, PhD; Keizo Kaneko, MD; Takehide Ogihara, MD, PhD; Hisamitsu Ishihara, MD, PhD; Yuko Sato, PhD; Kenji Takikawa, BA; Norihisa Nishimichi, PhD; Haruo Matsuda, DVM, PhD; Tatsuya Sawamura, MD, PhD; Yoshitomo Oka, MD, PhD

Background—Several clinical studies of statin therapy have demonstrated that lowering low-density lipoprotein (LDL) cholesterol prevents atherosclerotic progression and decreases cardiovascular mortality. In addition, oxidized LDL (oxLDL) is suggested to play roles in the formation and progression of atherosclerosis. However, whether lowering oxLDL alone, rather than total LDL, affects atherogenesis remains unclear.

Methods and Results—To clarify the atherogenic impact of oxLDL, lectin-like oxLDL receptor 1 (LOX-1), an oxLDL receptor, was expressed ectopically in the liver with adenovirus administration in apolipoprotein E–deficient mice at 46 weeks of age. Hepatic LOX-1 expression enhanced hepatic oxLDL uptake, indicating functional expression of LOX-1 in the liver. Although plasma total cholesterol, triglyceride, and LDL cholesterol levels were unaffected, plasma oxLDL was markedly and transiently decreased in LOX-1 mice. In controls, atherosclerotic lesions, detected by Oil Red O staining, were markedly increased (by 38%) during the 4-week period after adenoviral administration. In contrast, atherosclerotic progression was almost completely inhibited by hepatic LOX-1 expression. In addition, plasma monocyte chemotactic protein-1 and lipid peroxide levels were decreased, whereas adiponectin was increased, suggesting decreased systemic oxidative stress. Thus, LOX1 expressed in the livers of apolipoprotein E–deficient mice transiently removes oxLDL from circulating blood and possibly decreases systemic oxidative stress, resulting in complete prevention of atherosclerotic progression despite the persistence of severe LDL hypercholesterolemia and hypertriglyceridemia.

Conclusions—OxLDL has a major atherogenic impact, and oxLDL removal is a promising therapeutic strategy against atherosclerosis. (***Circulation.* 2008;118:75-83.**)

Key Words: atherosclerosis ■ lipoproteins ■ oxidative stress ■ oxidized low-density lipoprotein

Atherosclerosis is the major factor underlying the increased incidence of coronary heart disease and central vascular disease in the industrialized world.[1] Low-density lipoprotein (LDL) cholesterol is considered a major factor in atherosclerosis development.[2] In this decade, several clinical studies of statin therapy have demonstrated the pivotal roles of lowering LDL cholesterol in preventing atherosclerotic progression and decreasing cardiovascular mortality.[3]

Clinical Perspective p 83

Oxidative stress might play critical roles in many diseases. In particular, oxidation of LDL might be a key step in the development of atherosclerosis.[4–6] Oxidized LDL (oxLDL) has been proposed to be involved in many atherogenic changes in the vascular wall such as expression of adhesion molecules, migration of macrophages and smooth muscle cells, release of chemokines,[7] and impairment of endothelial nitric oxide production.[8] Importantly, oxLDL is incorporated into macrophages via receptor-mediated endocytosis, leading to macrophage transformation into foam cells and thus the plaque formation of atherosclerotic lesions. Furthermore, oxLDL itself reportedly induces oxidative stress in endothelial cells, smooth muscle cells, and macrophages, resulting in a vicious cycle of atherogenic plaque formation.[9] However,

Received October 9, 2007; accepted April 18, 2008.

From the Division of Molecular Metabolism and Diabetes (Y.I., J.G., T.Y., J.I., Y.H., K.K., H.I., Y.O.) and Division of Advanced Therapeutics for Metabolic Diseases, Center for Translational and Advanced Animal Research (H.K., K.U., K.K., T.O.), Tohoku University Graduate School of Medicine, Sendai; Department of Vascular Physiology, National Cardiovascular Center Research Institute, Osaka (Y.S., T.S.); and Laboratory of Immunobiology, Department of Molecular and Applied Biosciences, Graduate School of Biosphere Science, Hiroshima University, Hiroshima (K.T., N.N., H.M.), Japan.

*Drs Ishigaki, Katagiri, and Gao contributed equally to this work.

The online Data Supplement, which contains a table, can be found with this article at http://circ.ahajournals.org/cgi/content/full/CIRCULATIONAHA.107.745174/DC1.

Correspondence to Hideki Katagiri, MD, PhD, Division of Advanced Therapeutics for Metabolic Diseases, Center for Translational and Advanced Animal Research, Tohoku University Graduate School of Medicine, 2-1 Seiryo-Machi, Aoba-Ku, Sendai 980-8575, Japan. E-mail katagiri@mail.tains.tohoku.ac.jp

Circulation **is available at http://circ.ahajournals.org** **DOI: 10.1161/CIRCULATIONAHA.107.745174**

the effectiveness of antioxidant therapy against atherosclerosis is controversial.[10–15] In addition, antioxidants may inhibit not only oxLDL formation but also many other oxidation-sensitive pathways. Therefore, it is unclear that the antiatherogenic effects of antioxidants, if any, are due to inhibition of oxLDL formation. Thus, whether lowering oxLDL alone, rather than total LDL, affects atherogenesis remains to be elucidated. Therefore, to directly clarify the impact of oxLDL on the development of atherosclerosis, we designed a strategy for removing oxLDL from the circulation in a murine hypercholesterolemia model: apolipoprotein E (apoE)-deficient mice.

Several receptors for oxLDL have been identified in recent years.[16–20] Lectin-like oxLDL receptor-1 (LOX-1) is one such receptor for oxLDL[21] and is expressed in atherosclerotic lesions, including endothelial cells, macrophages, and smooth muscle cells,[22] suggesting that LOX-1 actively incorporates oxLDL. Therefore, with the goal of removing oxLDL from the circulation, we ectopically expressed LOX-1 in the livers of apoE-deficient mice using an adenoviral gene transfer system.

Methods

Preparation of Recombinant Adenovirus

Recombinant adenovirus containing murine LOX-1 cDNA under the CAG promoter was constructed as described previously.[23,24] A recombinant adenovirus bearing the bacterial β-galactosidase gene (*lacZ*) was used as a control.[25]

Animals

Animal studies were conducted in accordance with the institutional guidelines for animal experiments at Tohoku University. ApoE-deficient mice[26] (The Jackson Laboratory, Bar Harbor, Me) were fed a standard chow. At 46 weeks of age, the baseline group of mice (n=9) were killed to determine the extent of established lesions at this age. Adenoviruses were administered intravenously at a dose of 2×10^8 plaque-forming units to 46-week-old apoE-deficient mice.

Blood Analysis

Plasma total cholesterol, triglyceride, and adiponectin levels were determined as described previously.[27] Plasma lipoproteins were analyzed by high-performance liquid chromatography with molecular sieve columns[28] (Skylight Biotech, Inc, Akita, Japan). The monocyte chemoattractant protein (MCP)-1 concentration was measured with an ELISA kit (R&D Systems, Minneapolis, Minn). Plasma alanine aminotransferase was measured with the transaminase test C (Wako Pure Chemicals, Osaka, Japan). Plasma levels of lipid peroxides were quantified with an LPO determiner (Kyowa Medex, Tokyo, Japan). OxLDL levels were measured with a sandwich ELISA. Murine plasma samples were applied to a plate coated with human soluble LOX-1 protein and detected with anti-apoB as the first antibody and goat anti-chicken IgG (H+L) (KPL, Inc, Gaithersburg, Md) as the detecting antibody. The reaction was developed with a tetramethylbenzidine peroxidase EIA substrate kit (Bio-Rad Laboratories, Hercules, Calif), and absorbance was measured at 450 nm.

Immunoblotting

Hepatic protein extracts (250 μg total protein) were boiled in Laemmli buffer containing 10 mmol/L dithiothreitol, subjected to SDS-PAGE, and transferred onto nitrocellulose filters. The filters were incubated with the murine LOX-1 antibody and then with anti-goat immunoglobulin G coupled to horseradish peroxidase. The immunoblots were visualized with an enhanced chemiluminescence detection kit (Amersham, Buckinghamshire, UK).

Hepatic Uptake of oxLDL

Human LDL ($1.006<d<1.063$ g/mL) was purified by ultracentrifugation and oxidized with $CuSO_4$,[29] followed by labeling with fluorescent lipid (1,1′-dioctadecyl-3,3,3′,3′-tetramethylindocarbocyanine perchlorate [DiI]) as described previously.[30] Thirty minutes after DiI-labeled oxLDL (12 μg) injection, murine livers were excised for the extraction of lipids and measurement of fluorescence as described previously,[31] and livers of mice with nonlabeled oxLDL injection also were examined immunohistochemically. Fluorescent intensities of tissue lysates were measured with a fluorescence spectrophotometer (F-2000, Hitachi, Tokyo, Japan).

Histological Analysis

Mouse livers and aortas were removed and rinsed with saline. The tissues were fixed with 10% formalin and embedded in paraffin. Tissue sections were cut at a thickness of 4 μm and stained with hematoxylin and eosin. For immunohistochemistry, the streptavidin-biotin method was performed with a Histofine SAB-PO kit (Nichirei, Tokyo, Japan).[32] Slides were deparaffinized and then autoclaved in citrate buffer for antigen retrieval, followed by incubation with antibodies to oxLDL (Calbiochem, San Diego, Calif), mac-3 (BD Bioscience, San Jose, Calif), and smooth muscle actin (Progen, Heidelberg, Germany). Finally, the slides were visualized by incubation with a substrate solution containing 3,3′-diaminobenzidine tetrahydrochloride.

Measurement of Atherosclerotic Lesions

The aortas were removed, cleaned, cut open with the luminal surface facing up, and then immersion fixed in 10% formalin in PBS. The inner aortic surfaces were stained with Oil Red O to visualize neutral lipid (cholesteryl ester and triglycerides) accumulation for 25 minutes at room temperature. After rinsing with 60% isopropyl alcohol and distilled water, the Oil Red O–stained areas were quantified by Scion Image software analysis (Scion Corp, Frederick, Md) of the digitized microscopic images. Results were expressed as percentages of the lipid-accumulating lesion area to the total aortic area analyzed.

Quantitative Real-Time Polymerase Chain Reaction–Based Gene Expression

On day 5 after adenoviral administration, total RNAs in 0.1 g of the aortas and livers from 24-week-old LacZ and LOX-1 mice were isolated with ISOGEN (Wako Pure Chemical Co, Osaka, Japan), and cDNA was synthesized with a Cloned AMV First Strand Synthesis Kit (Invitrogen, Rockville, Md) using 5 μg total RNA. cDNA synthesized from total RNA was evaluated with real-time quantitative polymerase chain reaction (LightCycler Quick System 350S, Roche Diagnostics GmbH, Mannheim, Germany). The relative amount of mRNA was calculated with GAPDH as the invariant control. The primers used are described in Table I of the online Data Supplement.

Statistical Analysis

All data are expressed as mean±SEM. All statistical analyses were performed with the Statistical Package for the Social Sciences version 13.0 (SPSS Japan Inc, Tokyo, Japan). Normality was tested with the Kolmogorov-Smirnov test. When data were normally distributed, the statistical significance of differences was assessed with the unpaired *t* test and 1-way ANOVA, followed by Tukey's post hoc analyses. The Mann–Whitney *U* test was applied when data were not normally distributed. Repeated-measures ANOVA was used to assess changes in plasma oxLDL values measured serially in time between the 2 experimental groups. In all analyses, values of $P<0.05$ were accepted as statistically significant.

The authors had full access to and take full responsibility for the integrity of the data. All authors have read and agree to the manuscript as written.

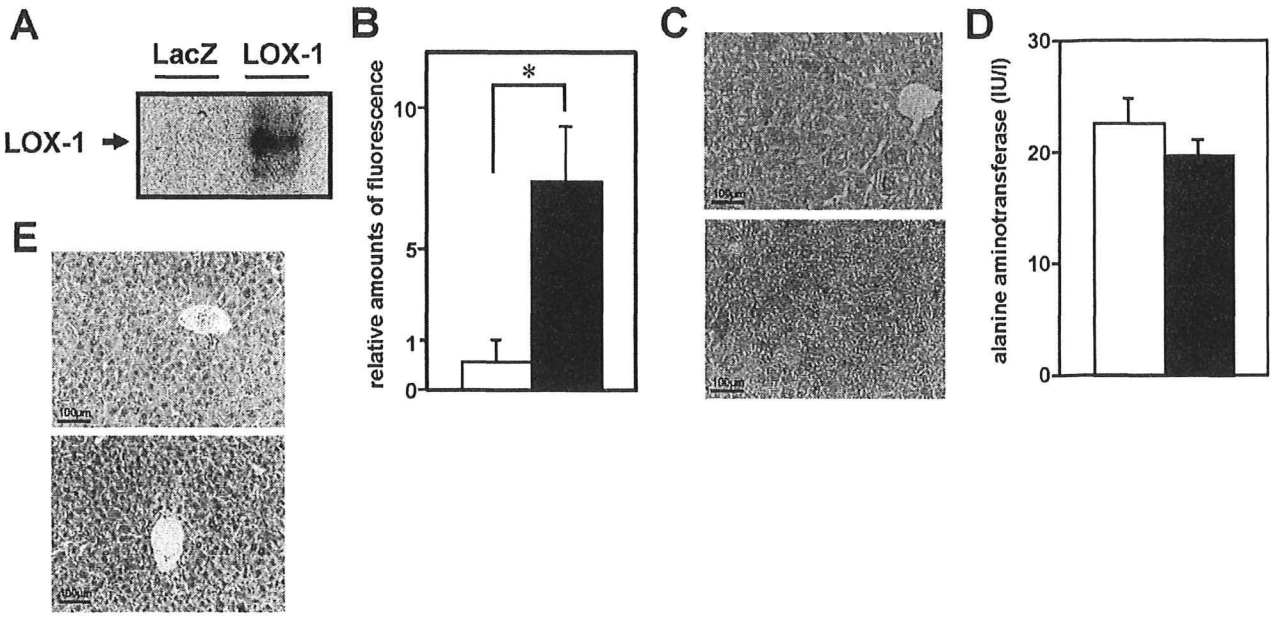

Figure 1. LOX-1 was ectopically and functionally expressed in the liver as an oxLDL receptor. A, Liver extracts were immunoblotted with anti–LOX-1 antibody 5 days after adenoviral administration. B, Mouse livers were removed 30 minutes after intravenous injection of DiI-labeled oxLDL, followed by measurement of fluorescent values in the livers of LacZ mice (white bars) and LOX-1 mice (black bars; n=5 per group). C, The livers of LacZ mice (top) and LOX-1 mice (bottom) were removed 30 minutes after intravenous oxLDL injection, followed by staining of hepatic sections with anti-oxLDL antibody. D, Plasma alanine aminotransferase levels were determined 5 days after adenoviral administration to LacZ mice (white bars) and LOX-1 mice (black bars; n=6 per group). E, The livers of LacZ mice (top) and LOX-1 mice (bottom) were stained with hematoxylin and eosin 4 weeks after adenoviral administration. B, D, Data are presented as mean±SE. *$P<0.05$.

Results

Adenoviruses encoding LOX-1 or LacZ cDNA were administered intravenously to apoE-deficient mice at 46 weeks of age. Mice of this age were chosen because atherosclerosis progresses dramatically during the period just before 1 year of age.[33] As we reported previously,[34] intravenous administration of recombinant adenoviruses results in selective transgene expression in the liver with no detectable expression in other tissues (data not shown). As shown in Figure 1A, administration of LOX-1 adenovirus induced LOX-1 expression in the livers of mice (LOX-1 mice), whereas no LOX-1 expression was detected in those of control mice given LacZ adenovirus (LacZ mice).

To examine hepatic uptake of oxLDL with ectopic expression of LOX-1, fluorescence-labeled oxLDL was injected intravenously, followed by measurement of fluorescence values in the liver. Hepatic fluorescence values were markedly increased in LOX-1 mice compared with LacZ mice (Figure 1B). In addition, 30 minutes after intravenous oxLDL injection, hepatic oxLDL deposition was demonstrated immunohistochemically with anti-oxLDL antibody (Figure 1C). Thus, LOX-1 was ectopically and functionally expressed in the liver as an oxLDL receptor. On the other hand, plasma alanine aminotransferase levels were similar in LacZ- and LOX-1 mice (Figure 1D). In addition, histological analyses revealed no apparent infiltration or structural changes in the livers of LOX-1 mice (Figure 1E). However, hepatic expression of antioxidant enzymes, ie, catalase and glutathione S-transferase, was significantly upregulated (Figure 2A), suggesting increased oxidative stress in hepatocytes. On the other hand, levels of C-reactive protein, interleukin-1β, and tumor necrosis factor-α expression were not significantly altered in the liver (Figure 2B). Thus, LOX-1 ectopically expressed in the livers of apoE-deficient mice functionally incorporated oxLDL into hepatocytes, possibly increasing oxidative stress, but liver damage was apparently limited.

Next, plasma lipid parameters were measured. Hepatic LOX-1 expression did not significantly alter plasma total cholesterol or triglyceride levels (Figure 3A). In addition, cholesterol contents of the LDL and high-density lipoprotein fractions were not significantly altered in LOX-1 mice compared with those in LacZ mice (Figure 3B). In marked contrast, plasma oxLDL levels were dramatically decreased in LOX-1 mice for 2 weeks but returned to control levels by 3 weeks after adenoviral administration (Figure 3C), probably because of decreased adenovirus-mediated transgene expression in the liver after 2 weeks, as reported previously.[27] Thus, adenovirus-mediated LOX-1 expression in the liver resulted in very transient and selective oxLDL removal from the circulation despite the persistence of severe hypercholesterolemia and hypertriglyceridemia induced by apoE deficiency.

To elucidate the effects of hepatic LOX-1 expression on atherosclerosis, the extents of atherosclerotic lesions were determined, as represented by the ratio of Oil Red O–positive areas to the entire aorta. Atherosclerotic lesions of LacZ mice increased markedly, by 38%, during the 4-week period after adenoviral administration (from 46 to 50 weeks of age) compared with those at baseline (46-week-old mice) (Figure 4A and 4B). In contrast, intriguingly, atherosclerotic lesion areas of LOX-1 mice were very similar to those at baseline

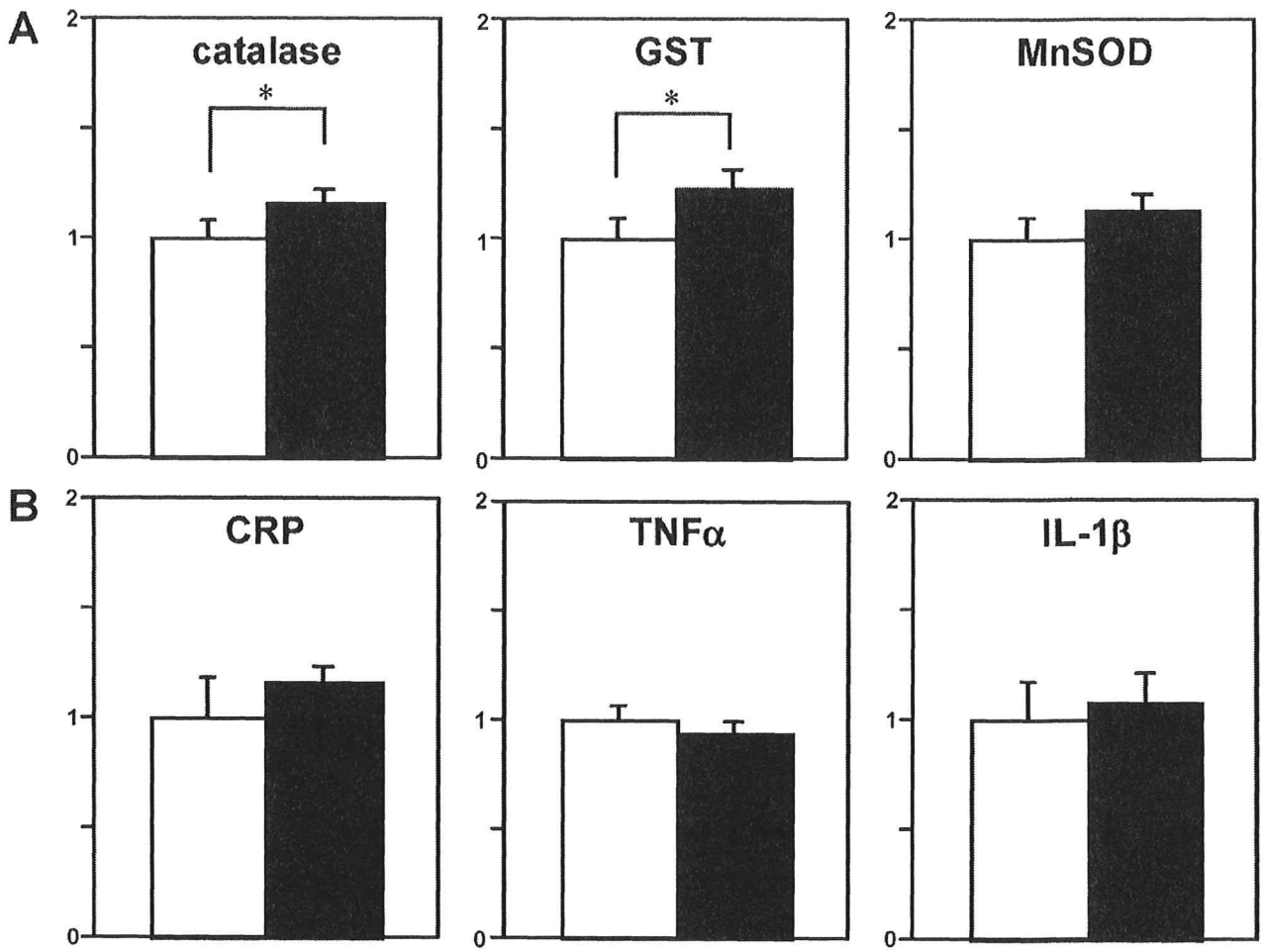

Figure 2. Relative amounts of mRNAs of proteins related to oxidative stress or inflammation in the liver. On day 5 after LacZ (white bars) or LOX-1 (black bars) adenovirus administration to 24-week-old apoE-deficient mice, relative amounts of mRNA of proteins related to oxidative stress (A) or inflammation (B) in the liver were determined by quantitative real-time polymerase chain reaction and corrected with GAPDH as the internal standard (n=9 in LacZ mice, n=11 in LOX-1 mice). Data are presented as mean±SE. GST indicates glutathione S-transferase; MnSOD, manganese superoxide dismutase; CRP, C-reactive protein; TNFα, tumor necrosis factor-α; and IL-1β, interleukin 1β. *P<0.05.

and were significantly smaller than those of LacZ mice (Figure 4A and 4B). These findings indicate that hepatic LOX-1 expression completely inhibited the progression of aortic atherosclerosis during the 4-week period when atherosclerosis markedly progresses in control apoE-deficient mice. Thus, oxLDL removal from circulating blood, even transient, exerts striking antiatherogenic effects, indicating the enormous impact of oxLDL on atherosclerosis.

Next, we immunohistochemically examined macrophage and smooth muscle cell infiltration into the plaques. Mac-3 staining revealed that macrophage deposition in established plaque lesions did not differ between LacZ- and LOX-1 mice (Figure 5A and 5B). In contrast, in LOX-1 mice, smooth muscle actin–positive areas in plaques were larger, especially in the surface areas of plaque lesions, than in LacZ mice. In LacZ mice, smooth muscle actin–positive areas in plaques were significantly decreased compared with those at baseline, and these decrements were inhibited by hepatic LOX-1 expression (Figure 5C and 5D). These findings suggest oxLDL removal from the circulation to inhibit the increase in vulnerability that occurs during plaque progression.

Furthermore, plasma MCP-1 levels were significantly lower in LOX-1 mice than in LacZ mice (Figure 6A). In contrast, plasma levels of adiponectin, which is considered a protective molecule against vascular damage,[35] were significantly higher in LOX-1 mice (Figure 6B). In addition, plasma lipid peroxide levels were markedly lower in LOX-1 mice (Figure 6C). Oxidative stress reportedly upregulates and downregulates MCP-1 in vascular cells[36] and adiponectin in adipocytes,[37] respectively. Taken together with the finding of decreased lipid peroxide levels, systemic oxidative stress is likely to be decreased in LOX-1 mice.

Then, we examined mRNA expressions of oxidative stress– and inflammation-related proteins in the aortas of 24-week-old LacZ and LOX-1 mice on day 5 after adenoviral administration. The antioxidant enzymes catalase, glutathione S-transferase, and manganese superoxide dismutase tended to be downregulated in the aortas of LOX-1 mice, although the differences did not reach statistical significance (Figure 7A). In addition, aortic expression of MCP-1, interleukin-6, and interleukin-1β was significantly decreased in LOX-1 mice (Figure 7B), indicating decreased oxidative stress and local

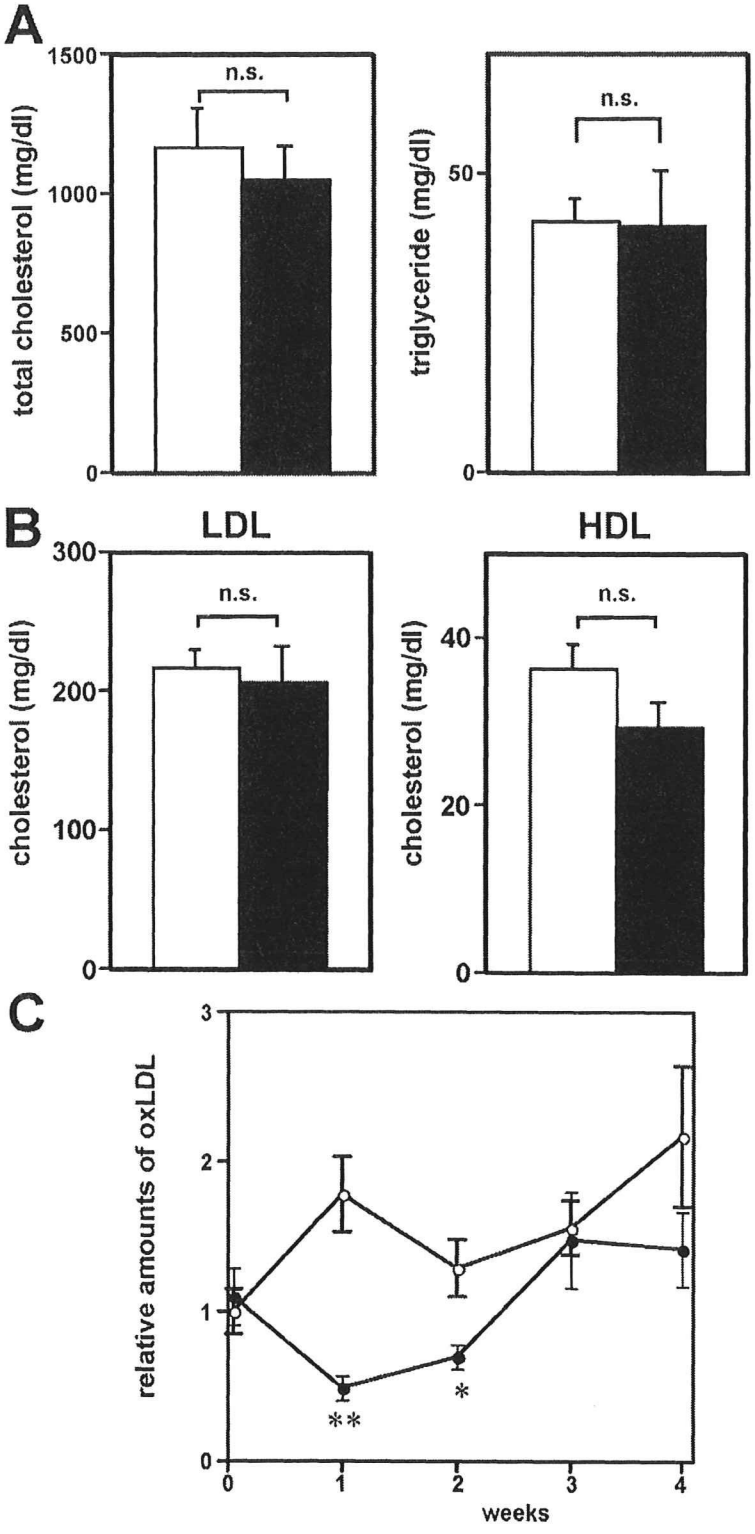

Figure 3. Hepatic LOX-1 expression transiently decreased plasma oxLDL without altering total cholesterol, triglyceride, or LDL cholesterol levels. A, Plasma total cholesterol (left) and triglyceride (right) levels of LacZ mice (white bars) and LOX-1 mice (black bars) were measured after a 10-hour fast 2 weeks after adenoviral administration (n=5 per group). B, Plasma samples (20 μL) from each mouse were separated and analyzed by high-performance liquid chromatography. Cholesterol contents of LDL and high-density lipoprotein (HDL) fractions were determined in LacZ mice (white bars) and LOX-1 mice after a 10-hour fast 2 weeks after adenoviral administration (black bars; n=3 per group). C, Plasma oxLDL levels were determined weekly until 4 weeks after adenoviral administration in LacZ mice (○) and LOX-1 mice (●; n=6 per group). Data are presented as mean±SE. $^*P<0.05$, $^{**}P<0.01$.

inflammation in the aortas of LOX-1 mice. OxLDL itself reportedly induces oxidative stress in endothelial cells, smooth muscle cells, and macrophages, resulting in a vicious cycle of atherogenic plaque formation.[9] Taken together, these results show that oxLDL removal from circulating blood may decrease systemic oxidative stress and inflammatory responses by blocking this vicious cycle, thereby exerting further beneficial effects against atherosclerosis.

Discussion

Several clinical studies have shown that lowering LDL cholesterol inhibits the progression of atherosclerosis.[3] The

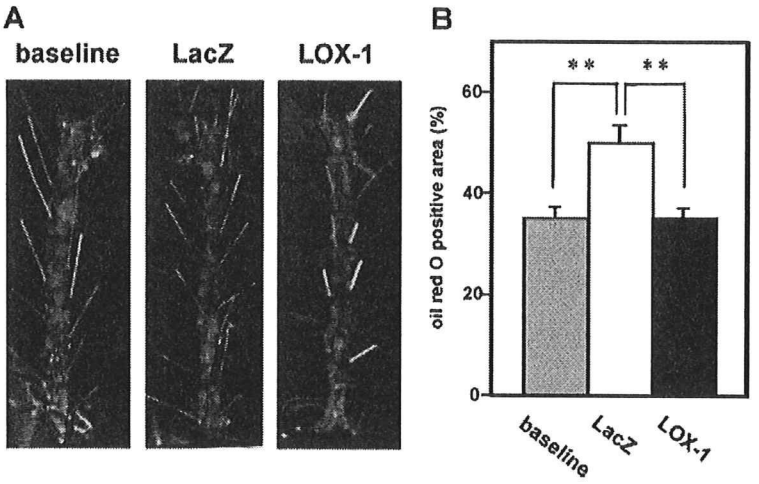

Figure 4. Hepatic LOX-1 expression completely inhibited atherosclerosis progression. A, Aortic atherosclerosis was evaluated as the Oil Red O–positive area. B, The Oil Red O–positive areas were quantified and expressed as percentages of the total aortic area in baseline (46-week-old) mice (gray bars; n=9), 50-week-old LacZ mice (white bars; n=13), and 50-week-old LOX-1 mice (black bars; n=13). Representative histological findings of the whole aorta are shown in A. Data are presented as mean±SE. $^{**}P<0.01$.

beneficial effects of statin therapy for reducing both atherogenic lipoproteins and cardiovascular mortality have been established in this decade. In the present study, despite not altering plasma LDL cholesterol levels, hepatic LOX-1 expression completely inhibited atherosclerotic progression. Thus, oxLDL, but not other LDL fractions, is likely to have a major impact on atherosclerosis development.

In recent reports, LDL cholesterol reduction was shown not only to inhibit coronary atheroma progression[38] but also to induce regression of thoracic aortic plaques, as evaluated by magnetic resonance imaging.[39] Moreover, aggressive lipid-lowering therapy, ie, LDL cholesterol removal, with LDL apheresis produced remarkable regression of coronary atherosclerotic plaques.[40] Here, in LOX-1 mice, atherosclerotic progression was completely inhibited despite a very transient oxLDL decrease, suggesting not only preventive but also therapeutic effects of oxLDL removal. In addition, smooth muscle cells persisted in plaques, particularly in plaque

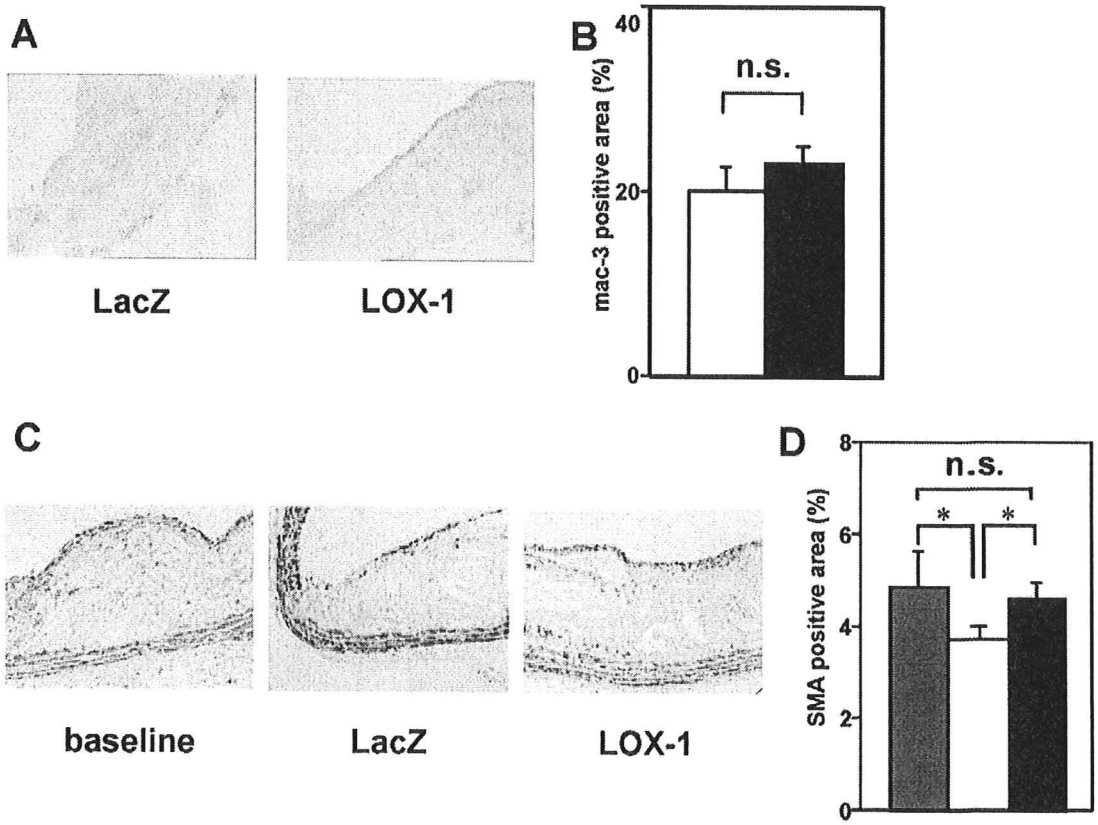

Figure 5. Macrophages and smooth muscle cells in established plaques of LOX-1 mice. A, B, Macrophage depositions were determined immunohistochemically with anti-macrophage (mac-3) antibody (A), and positive areas were measured as the lesion percentage of whole plaques (B). C, D, Smooth muscle cell infiltration was determined immunohistochemically with anti-smooth muscle actin (SMA) antibody (C), and positive areas were measured as the lesion percentage of whole plaques (D). Representative histological findings of the plaque are shown in A and C.

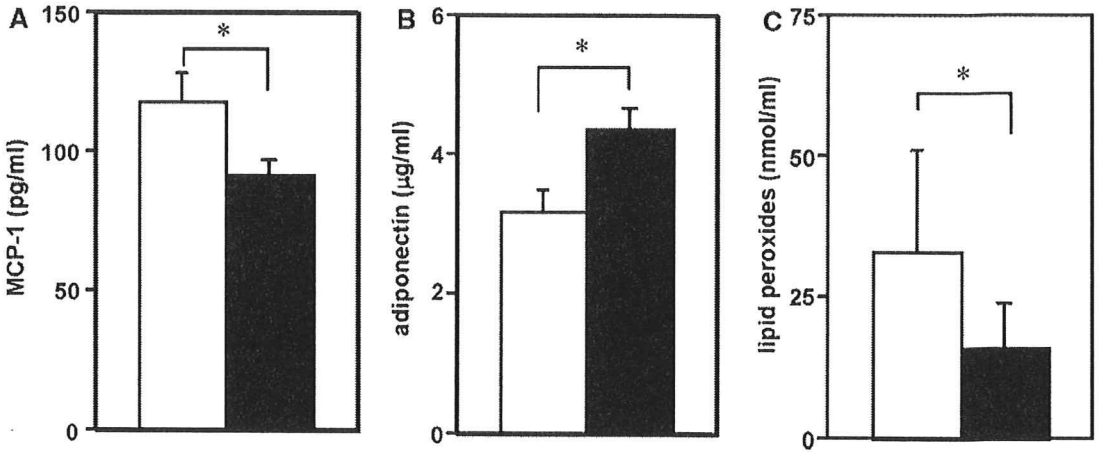

Figure 6. Hepatic LOX-1 expression altered oxidative stress–related plasma parameters. Plasma monocyte chemotactic protein-1 (A), adiponectin (B), and lipid peroxide (C) levels were determined 2 weeks after adenoviral administration to LacZ mice (white bars) and LOX-1 mice (black bars; n=6 per group). Data are presented as mean±SE. *$P<0.05$.

surface areas of LOX-1 mice. OxLDL reportedly enhances apoptosis of smooth muscle cells.[41–43] Therefore, removal of oxLDL from circulating blood may affect the characteristics of plaque lesions by inhibiting apoptosis of smooth muscle cells infiltrating plaque lesions.

Intriguingly, the plasma level of adiponectin, which prevents atherosclerosis development and improves insulin sensitivity, increased with hepatic LOX-1 expression. It was reported that systemic oxidative stress correlates negatively with plasma adiponectin in human subjects[44] and decreases adiponectin expression in adipocytes.[37] On the other hand, plasma MCP-1 levels were suppressed in LOX-1 mice. Oxidative stress may induce MCP-1 upregulation in vascular smooth muscle cells, leading to atherosclerosis formation by

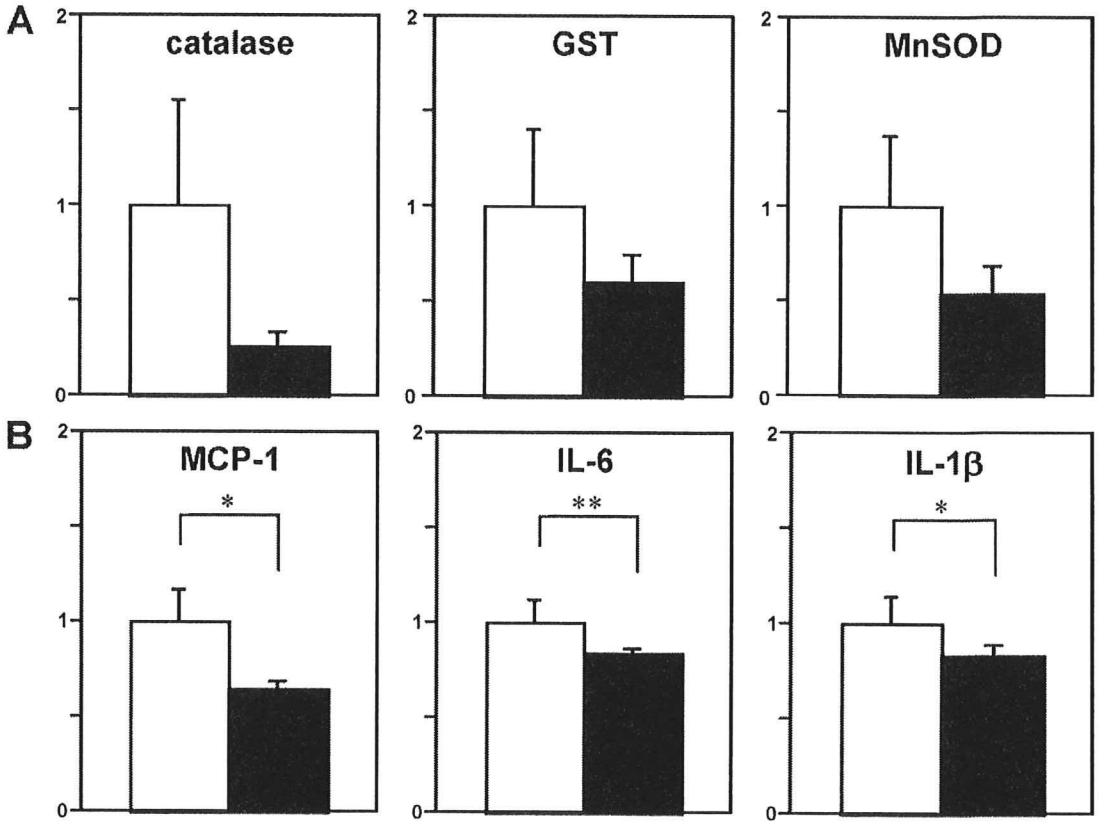

Figure 7. Relative amounts of mRNAs of proteins related to oxidative stress or inflammation in the aorta. On day 5 after LacZ (white bars) or LOX-1 (black bars) adenovirus administration to 24-week-old apoE-deficient mice, relative amounts of mRNA of proteins related to oxidative stress (A) or inflammation (B) in the aorta were determined by quantitative RT-PCR and corrected with GAPDH as the internal standard (n=9 in LacZ mice, n=11 in LOX-1 mice). Data are presented as mean±SE. GST indicates glutathione S-transferase; MnSOD, manganese superoxide dismutase; and IL-6, interleukin-6. *$P<0.05$, **$P<0.01$.

promoting recruitment of inflammatory cells to the vessel wall.[36] We cannot rule out the possibility that LOX-1 expressed in the liver scavenges other pro-oxidant molecules. However, it was reported that oxLDL itself potently induces oxidative stress.[9] Therefore, oxLDL removal from circulating blood is likely to decrease systemic oxidative stress, resulting in adiponectin upregulation and MCP-1 downregulation, thereby exerting further beneficial effects against atherosclerosis.

The effectiveness of antioxidant therapy against atherosclerosis is controversial.[10–15] In murine models, administration of antioxidants effectively reduces atherosclerosis.[12] On the other hand, most clinical trials yielded negative results.[15] This may be at least partly due to insufficient antioxidant effects of natural and synthetic compounds when administered to human subjects. In a randomized placebo-controlled study in healthy adults, daily administration of vitamin E at doses as high as 2 000 mg did not affect the breakdown of lipid peroxidation products despite a substantial increase in plasma vitamin E concentrations.[45] In addition, high doses of these antioxidants reportedly have adverse effects,[15] including the pro-oxidant effects of vitamin E at high doses.[46] Therefore, clinical application of these antioxidants seems to be limited. Thus, the present results provide a potential new therapeutic target because the antiatherogenic effect was observed after transient lowering of oxLDL.

Conclusions

LOX1 expressed in the liver transiently removes oxLDL from circulating blood without altering total cholesterol or LDL cholesterol levels and is likely to decrease systemic oxidative stress, resulting in complete inhibition of atherosclerosis development in aged apoE-deficient mice. This study provides strong evidence of the major atherogenic impact of oxLDL. Removal of oxLDL, even transiently, is a promising therapeutic strategy for blocking the vicious cycle that leads to atherosclerosis.

Acknowledgments

We thank I. Sato, J. Fushimi, K. Kawamura, M. Aizawa, M. Hoshi, and T. Takasugi for technical support.

Sources of Funding

This work was supported by Grants in Aid for Scientific Research (B2, 15390282 to Dr Katagiri and 19591031 to Dr Ishigaki) from the Ministry of Education, Science, Sports and Culture of Japan and by a Grant in Aid for Scientific Research (H19-genome-005) to Dr Oka from the Ministry of Health, Labor, and Welfare of Japan. This work also was supported by two 21st Century COE Programs (to Drs Katagiri and Oka) from the Ministry of Education, Science, Sports, and Culture.

Disclosures

None.

References

1. Katagiri H, Yamada T, Oka Y. Adiposity and cardiovascular disorders: disturbance of the regulatory system consisting of humoral and neuronal signals. *Circ Res.* 2007;101:27–39.
2. Brown MS, Goldstein JL. A receptor-mediated pathway for cholesterol homeostasis. *Science.* 1986;232:34–47.
3. Shepherd J, Cobbe SM, Ford I, Isles CG, Lorimer AR, MacFarlane PW, McKillop JH, Packard CJ. Prevention of coronary heart disease with pravastatin in men with hypercholesterolemia: West of Scotland Coronary Prevention Study Group. *N Engl J Med.* 1995;333:1301–1307.
4. Ross R. Atherosclerosis: an inflammatory disease. *N Engl J Med.* 1999; 340:115–126.
5. Yla-Herttuala S, Palinski W, Rosenfeld ME, Parthasarathy S, Carew TE, Butler S, Witztum JL, Steinberg D. Evidence for the presence of oxidatively modified low density lipoprotein in atherosclerotic lesions of rabbit and man. *J Clin Invest.* 1989;84:1086–1095.
6. Witztum JL, Steinberg D. Role of oxidized low density lipoprotein in atherogenesis. *J Clin Invest.* 1991;88:1785–1792.
7. Yui S, Sasaki T, Miyazaki A, Horiuchi S, Yamazaki M. Induction of murine macrophage growth by modified LDLs. *Arterioscler Thromb.* 1993;13:331–337.
8. Kugiyama K, Kerns SA, Morrisett JD, Roberts R, Henry PD. Impairment of endothelium-dependent arterial relaxation by lysolecithin in modified low-density lipoproteins. *Nature.* 1990;344:160–162.
9. Galle J, Hansen-Hagge T, Wanner C, Seibold S. Impact of oxidized low density lipoprotein on vascular cells. *Atherosclerosis.* 2006;185:219–226.
10. Meagher E, Rader DJ. Antioxidant therapy and atherosclerosis: animal and human studies. *Trends Cardiovasc Med.* 2001;11:162–165.
11. Rimm EB, Stampfer MJ. Antioxidants for vascular disease. *Med Clin North Am.* 2000;84:239–249.
12. Pratico D, Tangirala RK, Rader DJ, Rokach J, FitzGerald GA. Vitamin E suppresses isoprostane generation in vivo and reduces atherosclerosis in ApoE-deficient mice. *Nat Med.* 1998;4:1189–1192.
13. Terasawa Y, Ladha Z, Leonard SW, Morrow JD, Newland D, Sanan D, Packer L, Traber MG, Farese RV Jr. Increased atherosclerosis in hyperlipidemic mice deficient in alpha-tocopherol transfer protein and vitamin E. *Proc Natl Acad Sci U S A.* 2000;97:13830–13834.
14. Dietary supplementation with n-3 polyunsaturated fatty acids and vitamin E after myocardial infarction: results of the GISSI-Prevenzione trial: Gruppo Italiano per lo Studio della Sopravvivenza nell'Infarto miocardico. *Lancet.* 1999;354:447–455.
15. Miller ER 3rd, Pastor-Barriuso R, Dalal D, Riemersma RA, Appel LJ, Guallar E. Meta-analysis: high-dosage vitamin E supplementation may increase all-cause mortality. *Ann Intern Med.* 2005;142:37–46.
16. Kodama T, Freeman M, Rohrer L, Zabrecky J, Matsudaira P, Krieger M. Type I macrophage scavenger receptor contains alpha-helical and collagen-like coiled coils. *Nature.* 1990;343:531–535.
17. Endemann G, Stanton LW, Madden KS, Bryant CM, White RT, Protter AA. CD36 is a receptor for oxidized low density lipoprotein. *J Biol Chem.* 1993;268:11811–11816.
18. Krieger M, Acton S, Ashkenas J, Pearson A, Penman M, Resnick D. Molecular flypaper, host defense, and atherosclerosis: structure, binding properties, and functions of macrophage scavenger receptors. *J Biol Chem.* 1993;268:4569–4572.
19. Acton SL, Scherer PE, Lodish HF, Krieger M. Expression cloning of SR-BI, a CD36-related class B scavenger receptor. *J Biol Chem.* 1994; 269:21003–21009.
20. Ramprasad MP, Terpstra V, Kondratenko N, Quehenberger O, Steinberg D. Cell surface expression of mouse macrosialin and human CD68 and their role as macrophage receptors for oxidized low density lipoprotein. *Proc Natl Acad Sci U S A.* 1996;93:14833–14838.
21. Sawamura T, Kume N, Aoyama T, Moriwaki H, Hoshikawa H, Aiba Y, Tanaka T, Miwa S, Katsura Y, Kita T, Masaki T. An endothelial receptor for oxidized low-density lipoprotein. *Nature.* 1997;386:73–77.
22. Kume N, Murase T, Moriwaki H, Aoyama T, Sawamura T, Masaki T, Kita T. Inducible expression of lectin-like oxidized LDL receptor-1 in vascular endothelial cells. *Circ Res.* 1998;83:322–327.
23. Mizuguchi H, Kay MA. Efficient construction of a recombinant adenovirus vector by an improved in vitro ligation method. *Hum Gene Ther.* 1998;9:2577–2583.
24. Mizuguchi H, Kay MA. A simple method for constructing E1- and E1/E4-deleted recombinant adenoviral vectors. *Hum Gene Ther.* 1999; 10:2013–2017.
25. Katagiri H, Asano T, Ishihara H, Inukai K, Shibasaki Y, Kikuchi M, Yazaki Y, Oka Y. Overexpression of catalytic subunit p110alpha of phosphatidylinositol 3-kinase increases glucose transport activity with translocation of glucose transporters in 3T3-L1 adipocytes. *J Biol Chem.* 1996;271:16987–16990.
26. Zhang SH, Reddick RL, Piedrahita JA, Maeda N. Spontaneous hypercholesterolemia and arterial lesions in mice lacking apolipoprotein E. *Science.* 1992;258:468–471.

27. Ishigaki Y, Katagiri H, Yamada T, Ogihara T, Imai J, Uno K, Hasegawa Y, Gao J, Ishihara H, Shimosegawa T, Sakoda H, Asano T, Oka Y. Dissipating excess energy stored in the liver is a potential treatment strategy for diabetes associated with obesity. *Diabetes*. 2005;54:322–332.
28. Gao J, Katagiri H, Ishigaki Y, Yamada T, Ogihara T, Imai J, Uno K, Hasegawa Y, Kanzaki M, Yamamoto TT, Ishibashi S, Oka Y. Involvement of apolipoprotein E in excess fat accumulation and insulin resistance. *Diabetes*. 2007;56:24–33.
29. Innerarity TL, Pitas RE, Mahley RW. Lipoprotein-receptor interactions. *Methods Enzymol*. 1986;129:542–565.
30. Devaraj S, Hugou I, Jialal I. Alpha-tocopherol decreases CD36 expression in human monocyte-derived macrophages. *J Lipid Res*. 2001; 42:521–527.
31. Fujino T, Asaba H, Kang MJ, Ikeda Y, Sone H, Takada S, Kim DH, Ioka RX, Ono M, Tomoyori H, Okubo M, Murase T, Kamataki A, Yamamoto J, Magoori K, Takahashi S, Miyamoto Y, Oishi H, Nose M, Okazaki M, Usui S, Imaizumi K, Yanagisawa M, Sakai J, Yamamoto TT. Low-density lipoprotein receptor-related protein 5 (LRP5) is essential for normal cholesterol metabolism and glucose-induced insulin secretion. *Proc Natl Acad Sci U S A*. 2003;100:229–234.
32. Yamada T, Katagiri H, Ishigaki Y, Ogihara T, Imai J, Uno K, Hasegawa Y, Gao J, Ishihara H, Niijima A, Mano H, Aburatani H, Asano T, Oka Y. Signals from intra-abdominal fat modulate insulin and leptin sensitivity through different mechanisms: neuronal involvement in food-intake regulation. *Cell Metab*. 2006;3:223–229.
33. Reddick RL, Zhang SH, Maeda N. Atherosclerosis in mice lacking apo E: evaluation of lesional development and progression. *Arterioscler Thromb*. 1994;14:141–147.
34. Uno K, Katagiri H, Yamada T, Ishigaki Y, Ogihara T, Imai J, Hasegawa Y, Gao J, Kaneko K, Iwasaki H, Ishihara H, Sasano H, Inukai K, Mizuguchi H, Asano T, Shiota M, Nakazato M, Oka Y. Neuronal pathway from the liver modulates energy expenditure and systemic insulin sensitivity. *Science*. 2006;312:1656–1659.
35. Okamoto Y, Kihara S, Ouchi N, Nishida M, Arita Y, Kumada M, Ohashi K, Sakai N, Shimomura I, Kobayashi H, Terasaka N, Inaba T, Funahashi T, Matsuzawa Y. Adiponectin reduces atherosclerosis in apolipoprotein E–deficient mice. *Circulation*. 2002;106:2767–2770.
36. Cushing SD, Berliner JA, Valente AJ, Territo MC, Navab M, Parhami F, Gerrity R, Schwartz CJ, Fogelman AM. Minimally modified low density lipoprotein induces monocyte chemotactic protein 1 in human endothelial cells and smooth muscle cells. *Proc Natl Acad Sci U S A*. 1990;87: 5134–5138.
37. Soares AF, Guichardant M, Cozzone D, Bernoud-Hubac N, Bouzaidi-Tiali N, Lagarde M, Geloen A. Effects of oxidative stress on adiponectin secretion and lactate production in 3T3-L1 adipocytes. *Free Radic Biol Med*. 2005;38:882–889.
38. Nissen SE, Tuzcu EM, Schoenhagen P, Brown BG, Ganz P, Vogel RA, Crowe T, Howard G, Cooper CJ, Brodie B, Grines CL, DeMaria AN. Effect of intensive compared with moderate lipid-lowering therapy on progression of coronary atherosclerosis: a randomized controlled trial. *JAMA*. 2004;291:1071–1080.
39. Yonemura A, Momiyama Y, Fayad ZA, Ayaori M, Ohmori R, Higashi K, Kihara T, Sawada S, Iwamoto N, Ogura M, Taniguchi H, Kusuhara M, Nagata M, Nakamura H, Tamai S, Ohsuzu F. Effect of lipid-lowering therapy with atorvastatin on atherosclerotic aortic plaques detected by noninvasive magnetic resonance imaging. *J Am Coll Cardiol*. 2005;45: 733–742.
40. Matsuzaki M, Hiramori K, Imaizumi T, Kitabatake A, Hishida H, Nomura M, Fujii T, Sakuma I, Fukami K, Honda T, Ogawa H, Yamagishi M. Intravascular ultrasound evaluation of coronary plaque regression by low density lipoprotein-apheresis in familial hypercholesterolemia: the Low Density Lipoprotein-Apheresis Coronary Morphology and Reserve Trial (LACMART). *J Am Coll Cardiol*. 2002;40:220–227.
41. Jovinge S, Crisby M, Thyberg J, Nilsson J. DNA fragmentation and ultrastructural changes of degenerating cells in atherosclerotic lesions and smooth muscle cells exposed to oxidized LDL in vitro. *Arterioscler Thromb Vasc Biol*. 1997;17:2225–2231.
42. Nishio E, Arimura S, Watanabe Y. Oxidized LDL induces apoptosis in cultured smooth muscle cells: a possible role for 7-ketocholesterol. *Biochem Biophys Res Commun*. 1996;223:413–418.
43. Okura Y, Brink M, Itabe H, Scheidegger KJ, Kalangos A, Delafontaine P. Oxidized low-density lipoprotein is associated with apoptosis of vascular smooth muscle cells in human atherosclerotic plaques. *Circulation*. 2000; 102:2680–2686.
44. Furukawa S, Fujita T, Shimabukuro M, Iwaki M, Yamada Y, Nakajima Y, Nakayama O, Makishima M, Matsuda M, Shimomura I. Increased oxidative stress in obesity and its impact on metabolic syndrome. *J Clin Invest*. 2004;114:1752–1761.
45. Meagher EA, Barry OP, Lawson JA, Rokach J, FitzGerald GA. Effects of vitamin E on lipid peroxidation in healthy persons. *JAMA*. 2001;285: 1178–1182.
46. Bowry VW, Ingold KU, Stocker R. Vitamin E in human low-density lipoprotein: when and how this antioxidant becomes a pro-oxidant. *Biochem J*. 1992;288(pt 2):341–344.

CLINICAL PERSPECTIVE

A consensus has been reached that lowering plasma low-density lipoprotein (LDL) inhibits atherosclerosis progression. However, whether lowering plasma oxidized LDL (oxLDL) alone contributes to preventing atherosclerosis remains uncertain. The antiatherogenic effects of antioxidant therapy that may inhibit oxLDL formation are controversial because most clinical trials yielded negative results. Here, it has been shown that removal of oxLDL from the circulation has a very strong effect against atherosclerosis. In this study, lectin-like oxLDL receptor 1 (LOX-1), an oxLDL receptor, was expressed ectopically in the livers of apolipoprotein E–deficient mice (LOX-1 mice), using adenoviral gene transfer, to remove oxLDL from the circulation. Intriguingly, a transient decrease in plasma oxLDL, without affecting non-oxLDL cholesterol levels, completely inhibited atherosclerotic progression. Systemic oxidative stress was shown to be decreased in LOX-1 mice. Thus, oxLDL plays very important roles in atherosclerosis formation, and the underlying mechanisms may involve both direct (foam cell formation) and indirect (increased oxidative stress) effects. In addition, smooth muscle cells in the surface areas of atherosclerotic plaques were increased in LOX-1 mice, suggesting that oxLDL makes plaques vulnerable, possibly leading to plaque ruptures. Thus, the results of this study provide potential therapeutic targets for atherosclerosis, ie, treatments that would potently lower plasma oxLDL, including inhibition of oxLDL formation and removal of oxLDL from the circulation. These promising strategies may contribute to the prevention of not only atherosclerosis formation but also the development of acute coronary syndrome.

Biochemical and Biophysical Research Communications 369 (2008) 1204–1208

Contents lists available at ScienceDirect

Biochemical and Biophysical Research Communications

journal homepage: www.elsevier.com/locate/ybbrc

Identification of Glypican3 as a novel GLUT4-binding protein

Akihiko Taguchi [a], Masahiro Emoto [a], Shigeru Okuya [a,*], Naofumi Fukuda [a], Yoshitaka Nakamori [a], Mutsuko Miyazaki [a], Sachiko Miyamoto [a], Katsuya Tanabe [a], Hiroyuki Aburatani [b], Yoshitomo Oka [c], Yukio Tanizawa [a]

[a] Division of Endocrinology, Metabolism, Hematological Sciences and Therapeutics, Department of Bio-Signal Analysis, Yamaguchi University Graduate School of Medicine, 1-1-1 Minami-Kogushi, Ube, Yamaguchi, Japan
[b] Genome Science Division, Research Center for Advanced Science and Technology, University of Tokyo, Tokyo, Japan
[c] Division of Molecular Metabolism and Diabetes, Tohoku University Graduate School of Medicine, Sendai 980-8575, Japan

ARTICLE INFO

Article history:
Received 5 March 2008
Available online 14 March 2008

Keywords:
GLUT4
3T3-L1 Adipocytes
GPC3

ABSTRACT

Insulin stimulates glucose uptake in fat and muscle primarily by stimulating the translocation of vesicles containing facilitative glucose transporters, GLUT4, from intracellular compartments to the plasma membrane. Although cell surface externalization of GLUT4 is critical for glucose transport, the mechanism regulating cell surface GLUT4 remains unknown. Using a yeast two-hybrid screening system, we have screened GLUT4-binding proteins, and identified a novel glycosyl phosphatidyl inositol (GPI)-linked proteoglycan, Glypican3 (GPC3). We confirmed their interaction using immunoprecipitation and a GST pull-down assay. We also revealed that GPC3 and GLUT4 to co-localized at the plasma membrane, using immunofluorescent microscopy. Furthermore, we observed that glucose uptake in GPC3-overexpressing adipocytes was increased by 30% as compared to control cells. These findings suggest that GPC3 may play roles in glucose transport through GLUT4.

Insulin stimulation of glucose uptake into skeletal muscle and adipose tissue is achieved via the translocation of intracellular-sequestered GLUT4 protein to the cell surface membrane [1,2]. On the plasma membrane, GLUT4 proteins, responding to insulin stimulation, remain externalized for a certain period of time and facilitate glucose transport. Although cell surface externalization of GLUT4 is critical for glucose transport, the mechanism regulating cell surface GLUT4 remains largely unknown. We speculated that it would require a protein capable of interacting with the glucose transporter.

Over the past decade, several GLUT4-binding proteins, such as mUbc9 [3], TUG [4], DAXX [5], L-3-hydroxyacyl-CoA dehydrogenase [6], and carboxyl esterase [7], have been identified using the C-terminus region of GLUT4 as bait in either a two-hybrid system or an immobilized GST fusion protein pull-down experiment. For example, mUbc9 was demonstrated to regulate transporter degradation [3], whereas TUG was shown to modulate GLUT4 distribution [4]. However, the functions of other GLUT4-binding proteins are not fully understood. We speculated that a change in the three-dimensional structure of the GLUT4 partial sequence has made it difficult to identify and analyze functional GLUT4 binding proteins. Thus, we used full-length GLUT4 for screening, and thereby identified GPC3 as a GLUT4-binding protein.

GPC3 is one of the heparan sulfate proteoglycans that are anchored to the cell membrane by a glycosyl-phosphatidylinositol protein [8]. This family of proteins was shown to be related to morphogenesis and GPC3 was originally reported to be a negative regulator of cell proliferation as well as the progression of malignant tumors [9–13]. Herein, we report GPC3 as a newly identified GLUT4-binding protein. This is the first report describing a protein that acts directly on GLUT4 molecules at the plasma membrane.

Materials and methods

Antibodies. Mouse monoclonal GPC3 antibody was provided by Dr. Hiroyuki Aburatani (University of Tokyo, Japan). The following antibodies were used: anti-GLUT4 rabbit and goat, anti-GST (Santa Cruz Biotechnology, CA); anti-FLAG (M2) (Sigma); anti-Myc (9E10) (Convance, CA) and fluorescent-conjugated and horseradish peroxidase-conjugated secondary antibodies (Jackson Immuno-Research Laboratories).

Constructs. Mouse GPC3 cDNA was purchased from Open Biosystems (Huntsville, AL). Wild-type GPC3 was subcloned into a pGEX-6P1 (GE Healthcare Biosciences) vector. FLAG-tagged GPC3 and 4×Myc-tagged GLUT4-eGFP was subcloned into a pcDNA3 (Invitrogen) vector. All chemically synthesized and PCR-derived DNA sequences were verified by DNA sequencing.

Preparation of recombinant adenovirus vectors. Recombinant adenovirus encoding eGFP or FLAG-tagged GPC3 was constructed using the AdEasy adenovirus vector system according to the manufacturer's instructions (Startagene). All amplified viruses were stored at −80 °C. 3T3-L1 adipocytes were infected with recombinant adenovirus vectors encoding eGFP and FLAG-tagged GPC3 at a multiplicity of infection (m.o.i.) of 50.

* Corresponding author. Fax: +81 836 22 2342.
E-mail address: okuya@yamaguchi-u.ac.jp (S. Okuya).

0006-291X/$ - see front matter © 2008 Elsevier Inc. All rights reserved.
doi:10.1016/j.bbrc.2008.03.027

Cell culture. 3T3-L1 fibroblasts were grown in DMEM with 10% fetal bovine serum (FBS) at 37 °C. The cells (3–5 days post-confluent) were differentiated into adipocytes by incubation in the same DMEM containing 0.5 mM isobutylmethylxanthine, 0.25 μM dexamethasone, and 4 μg/ml insulin for 3 days, and then grown in DMEM with 10% FBS for an additional 3–6 days. Human hepatocellular carcinoma cell line HepG2 cells were cultured in Eagle's minimum essential medium (EMEM) with 10% FBS in at 37 °C.

Primary culture of mouse hepatocytes. Mouse hepatocytes were prepared from 5-month male C57BL/6J mice as described previously [14]. Isolated cells were seeded onto coverslips and allowed to recover for 24 h.

Yeast two-hybrid screening. The MATCHMAKER LexA Two-hybrid System (Clontech) was used for identification of GLUT4-binding proteins. As bait for screening, the vector pLexA-GLUT4 expressing a fusion protein composed of full-length rat GLUT4 linked to the DNA-binding domain was constructed. A rat adipocyte cDNA library already cloned into the pB42AD vector was obtained from Origene Technologies (Rockville, MD). Approximately 300 colonies showed activation of the yeast reporter gene, and 15 colonies showing dependence on the LexA-GLUT4 fusion protein for activation of the reporter gene were selected. Plasmids from positive clones were subsequently isolated from the yeast, transferred to E. coli, and sequenced. Full-length cDNA was obtained by 5′RACE (Rapid Amplification of cDNA End) using a kit (Clontech) and the GenBank/NCBI databases were screened for similar sequences using BLAST Search.

In vitro GST pull-down assay. GST fusion proteins of full-length GPC3 and GST alone were purified according to the manufacturer's instructions. GLUT4 protein was generated from Myc-tagged GLUT4-eGFP (four-Myc epitope-tags in the first exofacial loop and eGFP in the C-terminus) transfected 293 cells and further purified using anti-Myc antibody. These GST fusion proteins and purified 4×Myc-tagged GLUT4-eGFP were mixed in PBS and incubated at 4 °C for 4 h. The proteins were then pulled down with glutathione–sepharose beads (GE Healthcare Biosciences).

Immunoprecipitation and immunoblotting. Cells were lysed in lysis buffer [20 mM Hepes (pH 7.2), 100 mM NaCl, 1 mM EDTA, 25 mM NaF, 1 mM sodium vanadate, 1 mM benzamidine, 5 μg/ml leupeptin, 5 μg/ml aprotinin, 1 mM PMSF, and 1 mM DTT] and the protein concentration was measured with BCA protein assay reagent (Pierce, Rockford, IL). For immunoprecipitation, the cell lysate was pre-incubated with protein-G Sepharose at 4 °C for 30 min to remove non-specific bound proteins. Then, samples were incubated with primary antibody at 4 °C for 8–12 h followed by incubation with protein-G Sepharose. Lysates and immunoprecipitates were resolved by SDS–PAGE and transferred to a polyvinylidene difluoride (PVDF) membrane (GE Healthcare Biosciences). The membranes were incubated with appropriate antibodies.

Immunofluorescence microscopy. 3T3-L1 adipocytes, HepG2 cells, and primary hepatocytes were seeded onto coverslips and allowed to recover for 24–48 h. 3T3-L1 adipocytes were serum-starved for 4 h in DMEM, followed by incubation with or without 100 nM of insulin for 15 min at 37 °C. Then, all of the cells were fixed with 3.7% formaldehyde in PBS and permeabilized with buffer A (0.5% Triton X-100 and 1% FBS in PBS) for 15 min, and finally incubated for 2 h with primary antibodies at room temperature. The cells were washed and incubated with an appropriate secondary antibody, or rhodamine-conjugated wheat germ agglutinin (Molecular Probes, Inc.) as a counter staining of cell membrane and Golgi system. The coverslips were washed thoroughly and mounted on glass slides. Immunostained cells were observed at room temperature with a laser-scanning confocal microscope (LSM5 PASCAL; Carl Zeiss Inc.).

Plasma membrane sheet assay. Cell surface protein was assayed using plasma membrane lawns as described previously [15]. The cells were subsequently swollen using hypotonic buffer and sonicated to generate a lawn of plasma membrane fragments. The membranes were immunostained with anti-GPC3 and anti-GLUT4 antibody. These cells were observed by laser confocal microscopy.

2-Deoxy-glucose uptake. Differentiated adipocytes were prepared in 24-well plates. Cells were infected with the recombinant adenoviruses. Two days thereafter, the cells were serum-starved for 2 h at 37 °C in Krebs–Ringer phosphate buffer (130 mM NaCl, 5 mM KCl, 1.3 mM $CaCl_2$, 1.3 mM $MgSO_4$, and 10 mM Na_2HPO_4, pH 7.4). The cells were then stimulated with or without 100 nM of insulin for 15 min, and deoxy-glucose uptake was determined by 2-deoxy-D-[2,6^{3}H] glucose incorporation.

Results and discussion

Identification of GLUT4-binding proteins

Regulation of glucose uptake in muscle and adipose tissues by insulin is important for proper maintenance of blood glucose. This hormone stimulates translocation of the GLUT4 glucose transporter from the intracellular membrane to the cell surface. After translocation to the plasma membrane, GLUT4 remains on the cell surface temporarily and facilitates glucose transport. However, the mechanism regulating cell surface GLUT4 is still largely unknown. We hypothesized that it requires protein–protein interactions at the plasma membrane. We used the yeast two-hybrid screening system to identify proteins that interact physically with full-length GLUT4. As bait, we used full-length rat GLUT4 cDNA and, as prey, a rat adipose tissue cDNA library. After the first screening, we obtained more than 300 colonies. After a second screening, 15 colonies remained positive. Ultimately, nine colonies were left. Full-length cDNAs were obtained by 5′RACE. One of them was 100% identical to GPC3 [16], which was originally cloned as OCI-5, a GPI anchored membrane protein [17]. Since we also obtained mUbc9 [3], which was previously identified using the same method, our experimental procedure was thought to have worked correctly. The GPC3 sequence obtained with the yeast two-hybrid system was comprised of the residues from 521 to 597. In order to confirm the interaction between GLUT4 and GPC3, we employed the yeast two-hybrid system again; using full-length GLUT4 cDNA and full-length GPC3 cDNA as the bait and prey, respectively. We confirmed the LacZ signal indicating a direct interaction between GPC3 and GLUT4 (Fig. 1A). Next, we determined GPC3 protein expression using Western blot analysis. As shown in Fig. 1B, we detected high molecular weight form corresponding to the glycosylated GPC3 and bands corresponding to the non-glycosylated GPC3 core protein and its cleavage product of in 3T3-L1 adipocytes as in HepG2 cells. These data were consistent with the previous reports [11,13].

Intracellular localization of GPC3

The intracellular localization of GPC3 was observed in adipocytes by laser confocal microscopy. First, we determined GPC3 protein by immunofluorescent microscopy using our specific antibody against GPC3 in HepG2 cells and primary hepatocytes as a positive or negative control, respectively (Fig. 2A). As shown in Fig. 2B, most of the GPC3 was at the plasma membrane, as reported for other cell lines [17]. As expected, we observed co-localization of GLUT4 and GPC3 after insulin stimulation (Fig. 2B). Next, in order to confirm plasma membrane integrity, we prepared plasma membrane sheets from 3T3-L1 adipocytes, stained with anti-GPC3 and anti-GLUT4 antibodies, and then observed GPC3 expression by confocal microscopy (Fig. 2C). We observed that GLUT4 translocated to the plasma membrane in response to insulin stimulation. GPC3 localized at the plasma membrane on under both conditions, and merged more clearly with GLUT4 after insulin stimulation.

The results shown in Fig. 1A and Fig. 2 suggest that GPC3 interacted with GLUT4 at the plasma membrane.

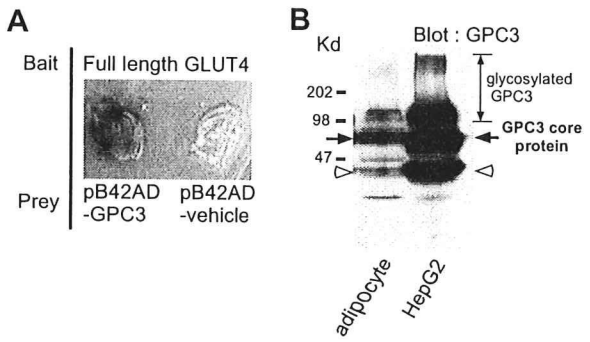

Fig. 1. Identification and expression profile of GPC3. (A) Interaction between GLUT4 and GPC3 was confirmed by the yeast two-hybrid system. Full-length cDNAs of GLUT4 and GPC3 were used as bait and prey, respectively. (B) Lysates of 3T3-L1 adipocytes and HepG2 cells were prepared, and separated by SDS-PAGE. The membrane was then blotted with anti-GPC3 antibody. HepG2 lysate was used as positive control. Arrow indicates the non-glycosylated full-length GPC3 core protein. Open arrowhead indicates a cleavage product containing the N-terminus of GPC3.

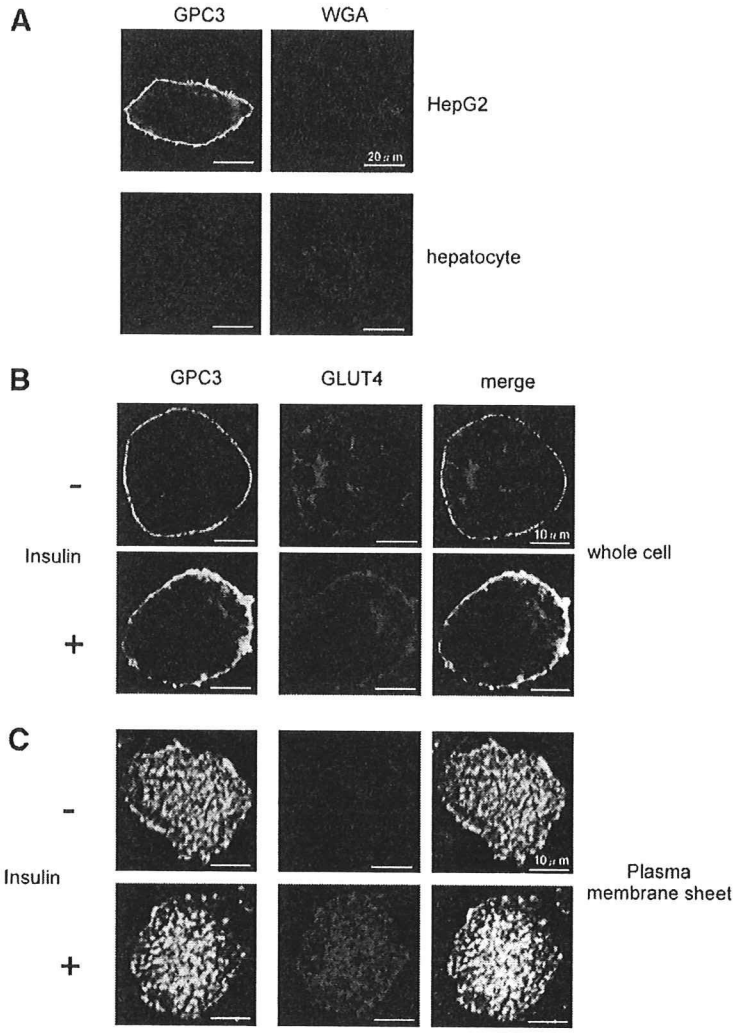

Fig. 2. Intracellular localization of GPC3. (A) Primary hepatocytes and HepG2 cells were plated on cover slips. These cells were fixed with formaldehyde and then stained using anti-GPC3 antibody followed by FITC-labeled secondary antibody. Rhodamine-conjugated wheat germ agglutinin (WGA) was used as counter staining of cell membrane and Golgi system. (B) 3T3-L1 adipocytes were serum-starved for 3-4 h and treated with or without 100 nM of insulin for 20 min. The cells were fixed with formaldehyde and stained using anti-GPC3 and anti-GLUT4 antibodies followed by appropriate FITC or Cy3 labeled secondary antibodies. These cells were observed by laser confocal microscopy. (C) 3T3-L1 adipocytes cultured on glass coverslips were treated with or without 100 nM of insulin for 15 min. At the end of each experiment, cells were rapidly washed in PBS followed by a 40 s treatment in PBS containing 0.5 mg/ml poly-L-lysine (Sigma). The cells were subsequently swollen using hypotonic buffer and sonicated to generate a lawn of plasma membrane fragments. The membranes were immunostained with anti-GPC3 and anti-GLUT4 antibody. Stained cells were observed using the confocal microscopy system as described above.

Interaction between GLUT4 and GPC3

In order to reconfirm the interaction between GPC3 and GLUT4, we conducted two other experiments; immunoprecipitation and a GST pull-down assay. First, we examined endogenous protein–protein interactions employing immunoprecipitation experiments. We prepared the total lysates of insulin-treated 3T3-L1 adipocytes. These lysates were immunoprecipitated with anti-GLUT4 antibody, and blotted with anti-GPC3 antibody. In adipocytes, we detected the interaction between GLUT4 and non-glycosylated GPC3 core protein (Fig. 3A). We also confirmed these interactions by immunoprecipitation with anti-GPC3 antibody (Fig. 3B). Second, we assessed the direct interaction between GLUT4 and GPC3 using the GST pull-down assay. We generated GST-GPC3 protein and GST alone using a bacterial system, and then purified these proteins with glutathione–sepharose beads. GLUT4 protein was purified from 293 cells transfected with 4×Myc-tagged-GLUT4-eGFP. These fusion proteins were mixed in PBS, and incubated for several hours. The proteins were then pulled down with glutathione–sepharose beads. We confirmed the GLUT4 signal in the GST-GPC3 precipitate lane, indicating a direct GLUT4 and GPC3 interaction in vitro (Fig. 3C).

Overexpression of GPC3 increased insulin stimulated glucose uptake

Since GPC3 was proved to GLUT4 at the plasma membrane, we examined whether GPC3 might regulate glucose uptake through GLUT4. We measured basal and insulin stimulated glucose uptake in 3T3-L1 adipocytes which transiently overexpressed GPC3 following transfection with adenovirus vectors. Overexpression of GPC3 increased insulin induced glucose uptake (Fig. 4). These data suggested that GPC3 overexpression to enhance insulin-stimulated glucose uptake via cell surface GLUT4.

Simpson–Golabi–Behmel syndrome (SGBS) is a rare, complex congenital syndrome with affected individuals having loss of function mutations in the GPC3 gene. Although many researchers

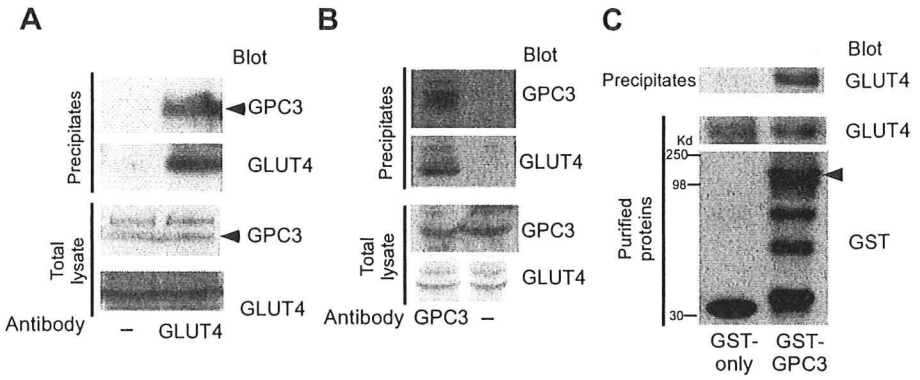

Fig. 3. GPC3 binds to GLUT4. (A) 3T3-L1 adipocytes were stimulated with 100 nM of insulin for 15 min. The lysates were incubated with or without anti-GLUT4 rabbit antibody followed by precipitation with protein A sepharose beads. Precipitates were separated by SDS–PAGE and immunoblotted with anti-GPC3 mouse monoclonal and anti-GLUT4 goat antibodies. Protein signals were visualized using horseradish peroxidase-conjugated secondary antibodies and an enhanced chemiluminescence substrate kit (GE Healthcare Biosciences). Arrowhead indicates GPC3 core protein. (B) 3T3-L1 adipocytes were stimulated with 100 nM of insulin for 15 min. Then, lysates of these adipocytes were immunoprecipitated using anti-GPC3 antibody or beads only. Precipitates were immunoblotted with anti-GLUT4 and anti-GPC3 antibodies for determination of GPC3-binding proteins. (C) GST-GPC3 and GST alone were bacterially expressed and purified by glutathione–sepharose beads. 4×Myc-tagged GLUT4-eGFP protein was expressed in 293 cells and purified using anti-Myc antibodies. Purified GST-GPC3 or GST proteins and GLUT4 protein were mixed and pulled down with glutathione–sepharose beads. The precipitates were separated by SDS–PAGE and analyzed by Western blotting using anti-GLUT4 and anti-GST antibodies. Arrowhead indicates full-length GST-GPC3.

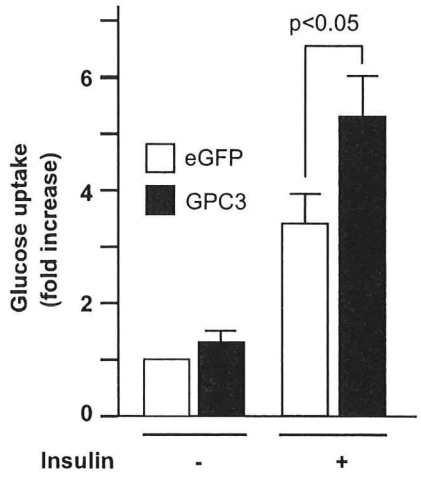

Fig. 4. Effect of GPC3 expression on glucose uptake 3T3-L1 adipocytes were infected with recombinant adenovirus vectors encoding FLAG-GPC3 or eGFP as a control at a m.o.i. of 50. The cells were serum-starved for 3 h and treated with or without 100 nM of insulin for 15 min. Glucose uptake was determined by 2-deoxy-D-[2,6^{3}H] glucose incorporation. Non-specific glucose uptake was measured in the presence of 20 μM cytochalasin B and subtracted from each determination to obtain the specific uptake. Statistical analyses were performed using Student's *t*-test. Experiments were repeated six times. Values are expressed as means ± SE, as indicated.

reported that the patients have general feature of overgrowth and cancer development, little is known about the clinical characteristics on glucose metabolism [18–21]. It was reported that some infants had hypoglycemia due to hyperplasia of islets of Langerhans rather than modification of insulin action in peripheral tissues [22]. More detailed analysis for the peripheral insulin action, especially on the adipose tissue would clarify the physiological role of GPC3 on glucose metabolism.

In conclusion, we identified a novel GLUT4-binding protein GPC3, using a yeast two-hybrid screening system. We also demonstrated GPC3 and GLUT4 to co-localized at the plasma membrane in response to insulin. Furthermore, overexpression of GPC3 increased insulin stimulated glucose uptake in cultured adipocytes. GPC3 may play a role in insulin stimulated glucose uptake.

Acknowledgments

We are also very grateful to Dr. Teruo Nishida for generously supporting us in the using a laser confocal microscope experiments. The authors thank Y. Kora and M. Kaneko for technical assistance. This study was supported in part by Grants-in-Aid for Scientific Research (17590934 to M. Emoto, 15590939 and 17590935 to S. Okuya) from the Ministry of Education, Culture, Sports, Science and Technology of Japan, and a grant from Takeda Science Foundation to S. Okuya.

References

[1] J.C. Hou, J.E. Pessin, Ins (endocytosis) and outs (exocytosis) of GLUT4 trafficking, Curr. Opin. Cell Biol. 19 (2007) 466–473.
[2] S. Huang, M.P. Czech, The GLUT4 glucose transporter, Cell Metab. 5 (2007) 237–252.
[3] F. Giorgino, O. de Robertis, L. Laviola, C. Montrone, S. Perrini, K.C. McCowen, R.J. Smith, The sentrin-conjugating enzyme mUbc9 interacts with GLUT4 and GLUT1 glucose transporters and regulates transporter levels in skeletal muscle cells, Proc. Natl. Acad. Sci. USA 97 (2000) 1125–1130.
[4] J.S. Bogan, N. Hendon, A.E. McKee, T.S. Tsao, H.F. Lodish, Functional cloning of TUG as a regulator of GLUT4 glucose transporter trafficking, Nature 425 (2003) 727–733.
[5] V.S. Lalioti, S. Vergarajauregui, D. Pulido, I.V. Sandoval, The insulin-sensitive glucose transporter, GLUT4, interacts physically with Daxx. Two proteins with capacity to bind Ubc9 and conjugated to SUMO1, J. Biol. Chem. 277 (2002) 19783–19791.
[6] Y. Shi, S.J. Samuel, W. Lee, C. Yu, W. Zhang, M. Lachaal, C.Y. Jung, Cloning of an L-3-hydroxyacyl-CoA dehydrogenase that interacts with the GLUT4 C-terminus, Arch. Biochem. Biophys. 363 (1999) 323–332.
[7] W. Lee, J. Ryu, J. Hah, T. Tsujita, C.Y. Jung, Association of carboxyl esterase with facilitative glucose transporter isoform 4 (GLUT4) intracellular compartments in rat adipocytes and its possible role in insulin-induced GLUT4 recruitment, J. Biol. Chem. 275 (2000) 10041–10046.
[8] J. Filmus, Glypicans in growth control and cancer, Glycobiology 11 (2001) 19R–23R.
[9] D.F. Cano-Gauci, H.H. Song, H. Yang, C. McKerlie, B. Choo, W. Shi, R. Pullano, T.D. Piscione, S. Grisaru, S. Soon, L. Sedlackova, A.K. Tanswell, T.W. Mak, H. Yeger, G.A. Lockwood, N.D. Rosenblum, J. Filmus, Glypican-3-deficient mice exhibit developmental overgrowth and some of the abnormalities typical of Simpson–Golabi–Behmel syndrome, J. Cell Biol. 146 (1999) 255–264.
[10] H. Lin, R. Huber, D. Schlessinger, P.J. Morin, Frequent silencing of the GPC3 gene in ovarian cancer cell lines, Cancer Res. 59 (1999) 807–810.
[11] Y. Midorikawa, S. Ishikawa, H. Iwanari, T. Imamura, H. Sakamoto, K. Miyazono, T. Kodama, M. Makuuchi, H. Aburatani, Glypican-3, overexpressed in hepatocellular carcinoma, modulates FGF2 and BMP-7 signaling, Int. J. Cancer 103 (2003) 455–465.
[12] H.H. Song, W. Shi, Y.Y. Xiang, J. Filmus, The loss of glypican-3 induces alterations in Wnt signaling, J. Biol. Chem. 280 (2005) 2116–2125.

[13] M.I. Capurro, W. Shi, S. Sandal, J. Filmus, Processing by convertases is not required for glypican-3-induced stimulation of hepatocellular carcinoma growth, J. Biol. Chem. 280 (2005) 41201–41206.
[14] J.D. Horton, H. Shimano, R.L. Hamilton, M.S. Brown, J.L. Goldstein, Disruption of LDL receptor gene in transgenic SREBP-1a mice unmasks hyperlipidemia resulting from production of lipid-rich VLDL, J. Clin. Invest. 103 (1999) 1067–1076.
[15] M. Emoto, S.E. Langille, M.P. Czech, A role for kinesin in insulin-stimulated GLUT4 glucose transporter translocation in 3T3-L1 adipocytes, J. Biol. Chem. 276 (2001) 10677–10682.
[16] J. Filmus, J.G. Church, R.N. Buick, Isolation of a cDNA corresponding to a developmentally regulated transcript in rat intestine, Mol. Cell. Biol. 8 (1988) 4243–4249.
[17] K. Watanabe, H. Yamada, Y. Yamaguchi, K-Glypican: a novel GPI-anchored heparan sulfate proteoglycan that is highly expressed in developing brain and kidney, J. Cell Biol. 130 (1995) 1207–1218.
[18] G. Pilia, R.M. Hughes-Benzie, A. MacKenzie, P. Baybayan, E.Y. Chen, R. Huber, G. Neri, A. Cao, A. Forabosco, D. Schlessinger, Mutations in GPC3, a glypican gene, cause the Simpson–Golabi–Behmel overgrowth syndrome, Nat. Genet. 12 (1996) 241–247.
[19] N. Okamoto, M. Yagi, K. Imura, Y. Wada, A clinical and molecular study of a patient with Simpson–Golabi–Behmel syndrome, J. Hum. Genet. 44 (1999) 327–329.
[20] S. Lindsay, M. Ireland, O. O'Brien, J. Clayton-Smith, J.A. Hurst, J. Mann, T. Cole, J. Sampson, S. Slaney, D. Schlessinger, J. Burn, G. Pilia, Large scale deletions in the GPC3 gene may account for a minority of cases of Simpson–Golabi–Behmel syndrome, J. Med. Genet. 34 (1997) 480–483.
[21] J.Y. Xuan, A. Besner, M. Ireland, R.M. Hughes-Benzie, A.E. MacKenzie, Mapping of Simpson–Golabi–Behmel syndrome to Xq25–q27, Hum. Mol. Genet. 3 (1994) 133–137.
[22] M.R. DeBaun, J. Ess, S. Saunders, Simpson–Golabi–Behmel syndrome: progress toward understanding the molecular basis for overgrowth, malformation, and cancer predisposition, Mol. Genet. Metab. 72 (2001) 279–286.

THE JOURNAL OF COMPARATIVE NEUROLOGY 510:1–23 (2008)

Wolfram Syndrome 1 (*Wfs1*) Gene Expression in the Normal Mouse Visual System

JUNE KAWANO,[1,2]* YUKIO TANIZAWA,[3] AND KOH SHINODA[2]
[1]Laboratory for Neuroanatomy, Department of Neurology, Kagoshima University Graduate School of Medical and Dental Sciences, Kagoshima, 890-8544, Japan
[2]Division of Neuroanatomy, Department of Neuroscience, Yamaguchi University School of Medicine, Ube, Yamaguchi, 755-8505, Japan
[3]Division of Endocrinology, Metabolism, Hematological Sciences and Therapeutics,Department of Bio-Signal Analysis, Yamaguchi University Graduate School of Medicine, Ube, Yamaguchi, 755-8505, Japan

ABSTRACT

Wolfram syndrome (OMIM 222300) is a neurodegenerative disorder defined by insulin-dependent diabetes mellitus and progressive optic atrophy. This syndrome has been attributed to mutations in the *WFS1* gene, which codes for a putative multi-spanning membrane glycoprotein of the endoplasmic reticulum. The function of WFS1 (wolframin), the distribution of this protein in the mammalian visual system, and the pathogenesis of optic atrophy in Wolfram syndrome are unclear. In this study we made a detailed analysis of the distribution of *Wfs1* mRNA and protein in the normal mouse visual system by using in situ hybridization and immunohistochemistry. The mRNA and protein were observed in the retina, optic nerve, and brain. In the retina, Wfs1 expression was strong in amacrine and Müller cells, and moderate in photoreceptors and horizontal cells. In addition, it was detectable in bipolar and retinal ganglion cells. Interestingly, moderate Wfs1 expression was seen in the optic nerve, particularly in astrocytes, while little Wfs1 was expressed in the optic chiasm or optic tract. In the brain, moderate Wfs1 expression was observed in the zonal, superficial gray, and intermediate gray layers of the superior colliculus, in the dorsomedial part of the suprachiasmatic nucleus, and in layer II of the primary and secondary visual cortices. Thus, *Wfs1* mRNA and protein were widely distributed in the normal mouse visual system. This evidence may provide clues as to the physiological role of Wfs1 protein in the biology of vision, and help to explain the selective vulnerability of the optic nerve to WFS1 loss-of-function. J. Comp. Neurol. 510:1–23, 2008.

Indexing terms: in situ hybridization; immunohistochemistry; retina; optic nerve; optic atrophy; wolframin; glutamine synthetase

Wolfram syndrome (OMIM 222300) is an autosomal recessive neurodegenerative disorder defined by juvenile-onset nonautoimmune insulin-dependent diabetes mellitus and progressive optic atrophy (Wolfram and Wagener, 1938). The nuclear gene responsible for Wolfram syndrome was mapped to human chromosome 4 at p16.1 (Polymeropoulos et al., 1994; Collier et al., 1996), and was subsequently identified as *WFS1* (Wolfram syndrome 1) or *wolframin* (Inoue et al., 1998; Strom et al., 1998). The *WFS1* gene encodes a putative 890-amino acid protein with an apparent molecular mass of ≈100 kDa (Inoue et al., 1998; Strom et al., 1998). The subcellular localization of WFS1 protein (wolframin) has been assigned primarily to the endoplasmic reticulum (ER) membrane. WFS1 protein contains nine transmembrane segments and is embedded in the ER membrane with the amino-terminus in the cytosol and the carboxy-terminus in the ER lumen (Takeda et al., 2001; Hofmann et al., 2003). Subsequent functional studies demonstrated that WFS1 protein is im-

Grant sponsor: Japan Society for the Promotion of Science (JSPS); Grant numbers: Grant-in-Aid for Scientific Research (C) (15591228 to J.K.); Grant-in-aid for Scientific Research (C) (17500231 to K.S.); Grant sponsor: The Ministry of Education, Culture, Sports, Science and Technology (MEXT); Grant number: Grant-in-aid for Scientific Research on Priority Areas (19040020 to K.S.); Grant sponsor: Kodama Memorial Fund Medical Research; Grant number: 2006-100 (to J.K.).

*Correspondence to: June Kawano, MD, PhD, Laboratory for Neuroanatomy, Department of Neurology, Kagoshima University Graduate School of Medical and Dental Sciences, 35-1, Sakuragaoka 8-chome, Kagoshima, 890-8544, Japan. E-mail: kawanoj@m2.kufm.kagoshima-u.ac.jp

Received 6 November 2006; Revised 3 June 2008; Accepted 20 March 2008

DOI 10.1002/cne.21734

Published online in Wiley InterScience (www.interscience.wiley.com).